博士論文

論文題目

Molecular mechanism underlying association of HLA-DQ with narcolepsy - Interaction of hypocretin-derived peptides with narcolepsy-associated HLA-DQ molecules -

（ヒト白血球抗原HLA-DQとナルコレプシー関連の分子機序に関する研究 -ハイポクレチンペプチドとナルコレプシー関連HLA-DQ分子の結合性-）

氏　　名　陳　萱容

Molecular mechanism underlying association of HLA-DQ with narcolepsy

- Interaction of hypocretin-derived peptides with narcolepsy-associated HLA-DQ molecules -

ヒト白血球抗原HLA-DQとナルコレプシー関連の分子機序に関する研究

—ハイポクレチンペプチドとナルコレプシー関連HLA-DQ分子の結合性—

指導教官 徳永 勝士 教授

東京大学 大学院医学系研究科

国際保健学専攻 人類遺伝学教室

平成 22 年度進学

学籍番号 41-117201

陳萱容

(HSUAN Jung CHEN)

APC	Antigen-presenting cell
BSA	Bovine serum albumin
CD	Cluster of differentiation
Cfu	Chemifluorescence
CHKB	Choline kinase B
CPT1B	Carnitine palmitoyltransferase 1B
CSF	Low cerebrospinal fluid
DMF	*N,N*-dimethylformamide
DMSO	Dimethyl sulfoxide
EBS	Epstein-Barr virus
EDS	Excessive daytime sleepiness
ER	Endoplasmic reticulum
FBS	Fetal bovine serum
GWAS	Genome-wide association studies
Hcrt	Hypocretin
HLA	Human leukocyte antigen
HRP	Horseradish peroxidase
mAb	Monoclonal antibody
MHC	Major histocompatibility complex
NAc	Nucleus accumbens
NTS	Nucleus of the solitary tract
NK cells	Natural killer cells
OXN	Orexin

PBMC	Peripheral blood mononuclear cell
PBS	Phosphate-buffered saline
PBST	Phosphate-buffered saline with Tween
PCR	Polymerase chain reaction
PE	Phycoerythrin
pMHC	Peptide-MHC
PVN	Paraventricular nucleus of the hypothalamus
P2Y11	Purinergic receptor subtype 2Y11
REM	Rapid eye movement
RFU	Relative fluorescence unit
PVDF	Polyvinylidene fluoride
SNP	Single nucleotide polymorphism
RT TCR	Room temperature T-cell receptor

Abstract:

The highly polymorphic *HLA* gene products are responsible for the presentation of peptide fragments as antigens to the immune system, and many autoimmune diseases are associated with HLA genes. A strong association of narcolepsy with HLA class II has been identified in previous studies, in which narcoleptic individuals of diverse ethnic backgrounds were found to carry a specific haplotype, *DQA1*01:02-DQB1*06:02*, suggesting that narcolepsy is an autoimmune disorder. Although the mechanism underlying autoimmunity in narcolepsy is not clear, hypocretin levels were found to be significantly decreased in narcoleptic patients, and hypocretin-producing cells were disrupted in the patients' brains. In addition, hypocretin deficiency has been detected in sporadic *HLA-DQB1*06:02*-positive adolescent-onset narcolepsy cases. Moreover, the *DQB1*06:01* and *DQB1*06:03* haplotypes are negatively associated with human narcolepsy, and *DQB1*06:04* is neutral for narcolepsy. No definitive evidence linking HLA to hypocretin deficiency has been found, and the underlying immunological mechanism remains elusive.

It has been hypothesized that autoimmune-triggered hypocretin loss is the major pathogenic factor for narcolepsy. The susceptible *HLA-DQA1*01:02-DQB1*06:02* haplotype product might recognize hypocretin, and therefore, mediate the autoimmune response. This hypothesis might explain why hypocretin-producing cells are destroyed in narcoleptic brain cells.

The crystal structure of hypocretin has been elucidated. However, the nature of the interactions between narcolepsy-associated HLA-DQ proteins and hypocretin-derived peptides has not been investigated. In this study, I constructed a *DQA1*01:02-DQB1*06:02* cell line that expresses narcolepsy-associated HLA-DQ molecules and evaluated the binding of these molecules to hypocretin-derived peptides in order to elucidate the autoimmune mechanism of narcolepsy. Subsequently, I determined the interactions between HLA combinations and variant hypocretin peptides by cell-based and plate-based methods. Cell lysates of HLA-DQA1*01:02-DQB1*06:02 (susceptible), DQA1*01:03-DQB1*06:01 (resistant), DQA1*01:03-DQB1*06:03 (resistant), and DQA1*01:02-DQB1*06:04 (neutral) were incubated with synthetic prepro-hypocretin-derived peptides, and their interactions were analyzed. Interactions between eight prepro-hypocretin-derived peptides and three different haplotype proteins related to narcolepsy were identified in this study. The binding affinities of different risk- and protective-HLA-DQ proteins with different hypocretin-derived peptides reported here provide insights into the role of hypocretin peptides in narcolepsy.

To the best of my knowledge, this is the first study to utilize a systematic binding assay to study the interactions between prepro-hypocretin-derived peptides and risk- and protective-narcolepsy haplotype HLA-DQ proteins. The plate-based peptide assay system is more efficient, sensitive, and specific than the cell-based assay. Therefore, the plate-based peptide assay is an ideal tool for screening autoantigens against the cell expression system in narcolepsy. My findings indicate that hypocretin peptides and the

immune system act as specific triggers of narcolepsy. However, from the binding study alone, it is not possible to conclude whether narcolepsy is an autoimmune disease. The results suggest that characterization of hypocretin peptides may help understand the epitopes involved in narcolepsy and provide insights into the pathogenic mechanism of narcolepsy.

1. INTRODUCTION

1. INTRODUCTION

1.1.Genetic factors, human leukocyte antigen, and narcolepsy

Human narcolepsy is a sleep disorder characterized by excessive daytime sleepiness, cataplexy, and abnormalities of rapid eye movement. The human leukocyte antigen (*HLA*) region is located at the chromosomal segment 6p21, and it encodes 252 expressed loci. *HLA* genes encode the major histocompatibility complexes (MHC) that present antigenic peptides to the T cell receptor (TCR). *HLA* gene products are expressed on the cell surface and present foreign and self-peptides to T cells (Figure 1). MHCs exhibit limited polymorphism for TCR repertoire development. The extent of polymorphism is determined by the specificity of the peptide binding site. Specific pockets on residues of MHC molecules are responsible for the different preferences of side chains of anchor residues. Understanding of MHC specificity towards a polymorphic peptide binding site and selection of TCR epitopes are essential to uncover the mechanisms underlying immune reactions to diseases.

Narcolepsy is associated with the *HLA class II* genes, *HLA-DR*, and *HLA-DQ*. Narcolepsy is associated with both *HLA-DR2* and *DQw1* in Japanese and Europeans (1-3), and *DR2* was the first specific genetic factor identified to be involved in narcolepsy (4-7). *DR2* has been detected in all narcoleptic patients of Japanese ethnicity but only in 20% of healthy individuals. However, *HLA-DQB1*06:02* was found to be a better marker than *DR2* for narcolepsy across all ethnic groups, suggesting that *DR2* is not the causal allele (8). Majority (90%) of narcolepsy patients of Caucasian and African American ethnicity possessed the *DQB1*06:02* allele.

Subsequently, the *DQB1*06:02* allele was identified as the strongest genetic risk factor for narcolepsy (9). Narcoleptic patients carry the *HLA-DQB1*06:02* allele in combination with *HLA-DR2* (9, 10). Another predisposition allele, *DQB1*03:01,* is also associated with narcolepsy (11). Conversely, *HLA-DQB1*06:01*, *DQB1*05:01*, *DQA1*01* (non-*DQA1*01:02*), and *DQB1*06:03* (9, 12) have been identified as protective alleles. The MHC of HLA-DQA1*01:02, HLA-DQA1*01:03, HLA-DQB1*06:01, HLA-DQB1*06:01, HLA-DQB1*06:01, HLA-DQB1*06:01, and HLA-DQB1*06:01 is responsible for the specific pockets on residues of different preferences of side chains of anchor residues (Tables 1, 2)

1.2. Other genetic factors associated with narcolepsy

In a previous genome-wide association study (GWAS), a single nucleotide polymorphism (SNP) located between carnitine palmitoyltransferase 1B (*CPT1B*) and choline kinase B was identified as a common variant that predisposes an individual to narcolepsy (13, 14). CPT1B is an enzyme of the β-oxidation pathway that may be involved in the regulation of theta oscillations during rapid eye movement (REM) sleep (15). Purinergic receptor subtype 2Y11 (*P2RY11*) is a crucial regulator of immune cell survival (13, 16, 17, 18). Low *P2RY11* expression in narcolepsy is associated with *P2RY11*-mediated resistance-reduced ATP-induced cell death in T lymphocytes and natural killer cells in the immune system (16, 19).

1.3. Major histocompatibility complex (MHC) and immune reactions

Unlike the T cell recombination mechanism, MHC polymorphism is inherited across generations; MHC plays an important role in the detection of pathogens. MHC

molecules are divided into MHC classes I and II. Peptide-MHC (pMHC) class I is transported to the cell surface to be recognized by T cells, and an immune reaction occurs when CD8 (+) T cells are activated (Fig. 1[A]). pMHC class II complex is transported to the cell surface, and is recognized by CD4 (+) T cells (Fig 1, [B, C]). In the thymus, T cells recognize peptides bound to MHCs, and T-cell precursors differentiate into immature T cells (20). pMHC density contributes to the outcome of positive and negative T cell selection (21, 22). Polymorphic MHC plays an important role in the immune system. Polymorphic MHC alters the specificity of peptide binding sites and influences the selection of TCR specificities during T cell repertoire development. The MHC class I molecule has a closed binding groove that restricts the length of peptides that can be bound in its peptide-binding groove to 8–11 peptide residues, whereas the MHC class II molecule has an open binding groove, which allows greater flexibility in its peptide-binding groove, as the length of bound peptides can be 9–25 bound peptide residues.

1.4. Hypocretin and narcolepsy

Hypocretin peptides are synthesized exclusively in the dorsomedial, perifornical, and lateral hypothalamus. Hypocretin (orexin) is a hypothalamic neuropeptide that regulates sleep and arousal states. The name “hypocretin” is derived from “secretin”; hypocretin is expressed in the hypothalamus but not in the cerebellum or hippocampus (23). There are two types of hypocretin peptides, hypocretin-1 and -2. The two types represent a pair of neuropeptides that are encoded by the prepro-hypocretin gene, and they interact with G protein-coupled receptors, namely hypocretin-1 and hypocretin-2

receptors (24). Hypocretin-1 and -2 are generated from prepro-hypocretin through a processing procedure that presumably involves prohormone convertases. Hypocretin-1 is a 33-amino acid peptide of 3.5 kDa with 2 sets of disulfide bonds, an N-terminal pyroglutamyl residue, and a C-terminal amidation (24). Hypocretin-2 is a 28-amino acid linear peptide of 2.9 kDa with a C-terminal amidation.

The hypocretin biosynthetic process involves efficient cleavage by a signal peptide peptidase in the endoplasmic reticulum and modification in the Golgi apparatus. The peptides are then transported to the axon terminal and stored in secretory vesicles. The mature peptide contains signal peptide cleavage sites. The amino-acid sequence of hypocretin-1 starts with Gln33, which is cyclized enzymatically into a pyroglutamyl residue by transamidation, and ends with an amidated C-terminus. Hypocretin-2 is composed of residues Arg69–Met96 (25).

Similar to other neuropeptides, hypocretin peptides are released into the synaptic uptake system. In a previous study, preprohypocretin mRNA and hypocretin-1 levels were found to be lowest at the beginning of the active phase, and the levels increased gradually towards the end of the active phase in rats (26). During the resting phase, preprohypocretin mRNA and hypocretin-1 were highest at the beginning of the active phase and decreased gradually thereafter (27). These results suggested that preprohypocretin mRNA regulates the sleep cycle. A hypothalamus-specific mRNA encodes hypocretin peptides, which are synaptically coupled with hypothalamic neurons. Hypocretin mRNA has been detected only in the brain and brain-associated hypocretin-positive nerve fibers. These neurons send excitatory projections to the

nucleus accumbens (NAc), nucleus of the solitary tract (NTS), and paraventricular nucleus of the hypothalamus (PVN); hypocretin peptides function as neurotransmitters that are exclusively expressed in the perifornical area (28).

The number of hypocretin neurons is 85%–95% lower in narcoleptic patients than in healthy individuals, and narcoleptics exhibit decreased expression levels of hypocretin peptides (29). These patients experience loss of orexin neurons in their hypothalamus, a portion of the brain that regulates sleep and appetite (30). Hypocretin (orexin) deficiency and low cerebrospinal fluid (CSF) hypocretin levels are often used to diagnose narcolepsy (29, 31). In animal models, the hypocretin-2 receptor gene was found to be mutated in canine narcolepsy, and preprohypocretin-knockout mice exhibited pathological changes similar to narcolepsy (32). However, only one human patient with a mutation of the hypocretin-2 receptor has been reported to date (33-35).

Hypocretin deficiency is found in sporadic *HLA-DQB1*06:02*-positive adolescent-onset narcolepsy cases. In narcoleptic patients, loss of hypocretin-producing cells in the brain has been identified as a common feature (36, 37). It has been hypothesized that autoimmune-triggered hypocretin loss is a major pathogenic factor for narcolepsy, and that the susceptible HLA-DQA1*01:02-DQB1*06:02 haplotype, rather than DR2 protein, might recognize hypocretin peptide or other antigens and mediate the autoimmune response (32, 36, 37).

Several hypothetical mechanisms have been suggested for the pathogenesis of narcolepsy. In previous studies, hypocretin peptides have been detected in the brain and

brain-associated hypocretin-positive nerve fibers, where they function as neurotransmitters that are exclusively expressed in the perifornical area (28).

In the hypocretin signal peptide, the hypocretin$_{1-13}$ side chains occupy the HLA-DQA1*01:02-DQB1*06:02 peptide-binding pockets (38). A hypothetical mechanism has been suggested for the pathogenesis of narcolepsy related to the hypocretin peptide (39). However, the pathological mechanism underlying the relationship between hypocretin peptide and HLA-DQ narcolepsy-associated haplotypes is still unknown. In addition, the binding of hypocretin$_{1-13}$ to DQ protein has not been discussed. There is a possibility that hypocretin peptide, specific antigens, or short candidate peptides that are presented by HLA proteins (MHCs) and recognized by CD4 (+) T cells may cause the death of hypocretin (orexin)-producing neurons, leading to decreased hypocretin peptide levels (36, 40, 41). It is plausible that hypocretin peptides, acting as neurotransmitters in the brain, bind to the HLA-DQA1*01:02-DQB1*06:02 protein and HLA-DQ protein associated with narcolepsy, thereby triggering an immune reaction.

1.5. Hypothetical mechanisms underlying autoimmunity and narcolepsy

Narcolepsy has been considered an immune-mediated disease, but the mechanism underlying the specific loss of hypothalamic hypocretin-producing neurons remains unknown. It has been hypothesized that narcolepsy is an autoimmune disorder because numerous HLA-associated disorders are also immune-mediated (32, 41) It has been hypothesized that destruction of most of the hypocretin-producing neurons in the hypothalamus because hypocretin peptides specifically expressed in the hypothalamus

are presented by HLA-DQA1*01:02-DQB1*06:02, which is recognized by T cells, resulting in an autoimmune response (Figure 2). However, narcolepsy is not consistent with a typical autoimmune disorder because autoantibodies have not been detected in individuals with the disease. Some groups have attempted to identify autoantibodies; however, narcolepsy-related serum autoantibodies have not been detected in patients with narcolepsy (42, 43). However, narcolepsy symptoms occur upon injection of serum from narcoleptic patients into mice (44).

Streptococcal infection is a potential trigger for narcolepsy (45); however, no correlation has been observed between the streptococcal antibody level and narcolepsy (46-49). Recently, anti-TRIB 2 autoantibodies were detected in narcoleptic patients (50, 51). Incidence of narcolepsy has also been reported in children and young adults who received the AS03-adjuvanted pandemic A/H1N1 2009 influenza vaccine in 2010 in Sweden and Finland (52-55). Increased cases of narcolepsy in AS03-adjuvanted pandemic A/H1N1 2009 influenza vaccine suggest a role for A/H1N1 influenza vaccine as the antigen in disease development. These observations of increased narcolepsy cases in individuals administered the AS03-adjuvanted H1N1 influenza vaccine indicate that narcolepsy might be an autoimmune disease (52, 54, 56-61). However, additional investigations are needed to better understand the factor(s) involved in narcolepsy in susceptible hosts.

1.6. Peptide-binding assay

Several assays have been developed over the years for the investigation of peptide–MHC interactions (62,63-65). Among these, cell-based and plate-based

peptide-binding assays are reliable methods to determine the binding affinity between HLA protein and peptides (66, 67, 68) and purified recombinant MHC molecules (69) on a spin column or enzyme-linked immunosorbent assay plate (70, 71). The complete set of antigenic peptides displayed on the MHC molecules is analyzed in order to map the MHC-peptide binding site (69, 72, 73). Previous studies have examined the binding of biotinylated peptides with competitor peptides to cells expressing the HLA molecules of interest on their surface, using fluorescently labeled reference peptides and unlabeled test peptides or purified MHC molecules (70, 74, 75).

1.7. Aim of the study

The binding of hypocretin peptides to different HLA-DQ proteins has not been studied comprehensively. To investigate the causal mechanism of narcolepsy, it is necessary to select an effective assay system for analyzing HLA class II molecules. The auto-antigen interacts with HLA class II molecules, thereby stimulating an autoimmune response to kill hypocretin-producing cells. The auto-antigen signal intensities for MHC class II have been widely studied in a cell-based peptide binding assay (81). I analyzed the interactions between narcolepsy-associated HLA-DQ proteins and hypocretin-derived peptides using a cell-based and plate-based peptide binding assay. The goal of the study was to identify a set of permissive site-specific amino acids that accommodate narcolepsy allele-specific binding and thus clarify the mechanism of narcolepsy. The purpose of this study was to develop an assay system to identify and examine synthetic peptides designed for prepro-hypocretin as potential autoantigens associated with the onset of narcolepsy. Mammalian NIH3T3 cells were used to

identify autoantigens that interact with proteins encoded by the *HLA-DQA1*01:02-DQB1*06:02* (susceptible), *DQA1*01:03-DQB1*06:01* (resistant), *DQA1*01:03-DQB1*06:03* (resistant), and *DQA1*01:02-DQB1*06:04* (neutral) haplotypes (Figure 3). These haplotype products share similar amino-acid residues in their auto-antigen binding motifs. This is the first study to analyze the differences in the auto-antigens and HLA class II DQ protein molecules encoded by narcolepsy risk, and identification of protective alleles might help identify the peptide epitopes involved in the autoimmune response to narcolepsy.

2. MATERIALS & METHODS

2. MATERIALS & METHODS

2.1. Plasmid construction

cDNAs of the narcolepsy-susceptible haplotype *HLA-DQA1*01:02-DQB1*06:02*, resistant haplotypes *DQA1*01:03-DQB1*06:01* and *DQA1*01:03-DQB1*06:03*, and neutral haplotype *DQA1*01:02-DQB1*06:04* fused with Step-tag II and His-tag were gifts from Dr. Hiroko Miyadera (Department of Human Genetics, University of Tokyo; Figure 3).

The cDNAs were ligated into the retroviral vector pMXs-neo using the restriction enzymes EcoRI (Nippon Gene Co., Ltd, Tokyo, Japan) and NotI (New England Biolabs) at the 5′ and 3′ ends, respectively. cDNA was confirmed by sequencing with an ABI 3130 sequencer; information regarding the primers has been provided in Table 3.

2.1.1. Establishment of a mammalian cell line that stably expresses DQ proteins

pMXs-neo/DQA1 and pMXs-puro/DQB1 were transfected into murine fibroblast cells (NIH3T3) obtained from the RIKEN BioResource Center Cell Bank (Tsukuba, Japan), by using retroviruses and packing cells (76) (Figure 3). pMXs vectors were provided by Dr. Toshio Kitamura (Institute of Medical Science, the University of Tokyo). pMXs-DQ plasmid (3 μg) was individually transfected into Plat-E cells, which were provided by Dr. Toshio Kitamura (Institute of Medical Science, the University of Tokyo) by using Opti-MEM® (Life Technologies Co., CA, USA) and FuGENE® HD Transfection Reagent (Promega Corporation, WI, USA). Plat-E cells were seeded in 6-cm plates and cultured in Dulbecco's Modified Eagle's

Medium (Sigma–Aldrich) with 10% FBS (Biological Industries Ltd.) and 1× L-glutamine (Wako Pure Chemical Industries Ltd.) at 37 °C and 5% CO_2. Plat-E cells were cultured for 24 h, and the medium was replaced. Supernatants containing retroviral particles were passed through a 0.45-μm filter (Sartorius K.K., Gottingen, Germany), and were added to NIH3T3 cells. DQA1 stable cell lines were established first; subsequently, the DQB1 genes were transduced into the DQA1 stable cell lines. NIH3T3 cells stably expressing *DQA1* and *DQB1* were then selected in the presence of puromycin (6 μg/mL; Merck K GaA, Darmstadt, Germany) and G418 (2 mg/mL) for 2 weeks.

For each stable cell line, surface expression of HLA-DQ proteins was confirmed by flow cytometry with fluorescein isothiocyanate (FITC)-conjugated anti-HLA-DR, DQ, and DPβ mAb (clone WR18, 10 μg/mL; Morphosys A.G., Munich, Germany) and isotypic control IgG2a-FITC (Beckman Coulter, Inc., US) antibodies. Plat-E cells were provided by Dr. Toshio Kitamura (Institute of Medical Science, University of Tokyo). NIH3T3 cells were obtained from the RIKEN Cell Bank (Tsukuba, Japan).

2.1.2. Confirmation of the expression of recombinant DQ proteins by dot-blot assay

For Strep-tag-based purification, DQA1*01:02-DQB1*06:02 cells (2×10^7 cells) were lysed in 400 μL of lysis buffer (0.5% w/w NP-40, 30 mM Na-phosphate pH 8.0, and 150 mM NaCl) in the presence of 1× Complete Protease Inhibitor Cocktail (Roche Diagnostics GmbH, Mannheim, Germany) and 1 μL of Benzonase® nuclease (0.05 U/μL; Merck KGaA, Darmstadt, Germany) on ice for 1 h. Then, 400 μL of cell lysate

was applied to a Strep-Tactin® spin column (IBA, USA). The column was washed with wash buffer (30 mM Na-phosphate, 150 mM NaCl, pH 8.0), and centrifuged for 30 s at 2000 rpm. Proteins were eluted using 60 μL of 2.5 mM biotin elution buffer (2.5 mM biotin, 100 mM Tris-HCl, 1 mM EDTA, and 150 mM NaCl).

For His-tag-based purification, DQA1*01:02-DQB1*06:02 cells (2×10^7 cells) were lysed in 400 μL of lysis buffer (0.5% (w/w) NP40, 30 mM Na-phosphate, and 150 mM NaCl, pH 8.0) in the presence of 1× Complete Protease Inhibitor Cocktail (Roche Diagnostics GmbH, Mannheim, Germany) and 1 μL of Benzonase® nuclease (0.05 U/μL; Merck KGaA, Darmstadt, Germany) on ice for 1 h. The cell lysate was diluted with the same volume of binding buffer (30 mM Na-phosphate, 150 mM NaCl pH 8.0), and 30 μL of anti-His tag beads (Medical & Biological Laboratories, Nagoya, Japan) was added. The beads were incubated for 30 min at RT, washed with wash buffer (30 mM Na-phosphate, 150 mM NaCl pH 8.0), and bound proteins were eluted with 60 μL of elution buffer ((0.25% NP-40, 30 mM Na-phosphate, 150 mM NaCl, and 0.2 M imidazole, pH 8.0).

For the dot-blot analysis, 5 μL of DQA1*01:02-DQB1*06:02 cell lysate was spotted onto a nitrocellulose membrane (GE Healthcare Co., Uppsala, Sweden), and left to dry for 12 h. The membrane was then blocked in 5% w/v bovine serum albumin (BSA) in phosphate-buffered saline with 0.05% w/w Tween 20 (PBST) for 1 h at RT in the dark and incubated with the primary antibody, anti-His tag mAb (clone 6C4, 1 μg/mL; Medical & Biological Laboratories Co., Aichi, Japan) at RT for 60 min. Subsequently, the membrane was washed 3 times with PBST at RT for 5 min and

incubated with 1/1000× HRP-conjugated goat anti-mouse IgG polyclonal antibody (final concentration, 0.04 μg/mL; Santa Cruz Biotechnology Inc., TX, USA) at RT for 60 min. The membrane was then washed 3 times with PBST and incubated with ECL™ Prime Western Blotting Detection Reagent (GE Healthcare Co., Uppsala, Sweden) for 5 min at RT. The intensity of chemifluorescence signals (cfu), which were analyzed using chemiluminescence signals recorded by the ChemiDoc™ XRS and Quantity One® software, respectively.

2.2. Cell-based peptide-binding assay

The peptide signal intensities for MHC class II have been widely studied in Epstein-Barr virus (EBV)-transformed cells. Untransfected DR1 with biotinylated $HA_{307-319}$ peptides were previously applied in a cell-based peptide binding assay (81). I analyzed the interactions between narcolepsy-associated HLA-DQ proteins and hypocretin-derived peptides using a cell-based peptide binding assay. The goal of the study was to identify a set of permissive site-specific amino acids that accommodate narcolepsy allele-specific binding and thus clarify the mechanism of narcolepsy. First, I used a cell-based peptide binding assay to characterize the autogenic peptide epitopes. In a preliminary experiment using the cell-based peptide binding assay, I selected an insulin peptide as the indicator peptide, and I used *HLA-DQA1*01:02-DQB1*06:02*- and *HLA-DQA1*01:02-DQB1*06:04*-expressing cell lines. In further studies, binding of hypocretin and other proteins that are expressed in hypocretin-producing cells to DQA1*01:02-DQB1*06:02 and other allele products will be tested. The goal of these studies will be to determine specific pockets on DQA1*01:02-DQB1*06:02 and

other residues of MHC molecules that are responsible for the different preferences for side chains of anchor residues based on different binding affinity.

2.2.1. Binding affinity of biotin to avidin, streptavidin, and anti-biotin antibody

The affinity of biotin for avidin, streptavidin, or anti-biotin antibody is quite strong. Nevertheless, nonspecific binding is a serious problem that is encountered when cell cultures are incubated with biotin-labeled peptides by flow cytometry. To avoid non-specific binding leading to misinterpretation of experimental results, the non-specific binding affinity of avidins that were obtained from various manufacturers and displayed on the NIH3T3 cell surface was examined. The binding affinity of the following avidins was examined: ExtrAvidin®−R-Phycoerythrin (E4011, Sigma Aldrich; excitation and emission wavelengths, 488 nm and 575 nm, respectively) (77), NeutrAvidin DyLight 550 (84606, Thermo Fisher Scientific); 562 nm and 576 nm), Streptavidin, R-Phycoerythrin (S866; Invitrogen; 566 nm and 575 nm), PE-anti-Biotin (409004; BioLegend, San Diego, CA; 488 nm and 575 nm), and PE-anti-Biotin (600-108-098; Rockland Immunochemicals Inc.; 488 nm and 575 nm) (78-80). Cells (5×10^5) were incubated with 0.01 μg/μL of the following reagents: ExtraAvidin (Sigma Aldrich) (77), NeutrAvidin DyLight 550 (Thermo Scientific), StrepAvidin-PE (Invitrogen), PE-anti-Biotin (BioLegend), and PE-anti-Biotin (Rockland), for 24 h at 37 °C. The samples were then washed with 500 μL of wash buffer and centrifuged at 7000 rpm. Signals for avidins were measured by flow cytometry. For NeutrAvidin DyLight 550, cell-surface binding of avidin was estimated at excitation and emission

wavelengths of 562 nm and 576 nm, respectively, and at concentrations of 50 μM, 150 μM, and 500 μM.

2.2.2. Cell-based peptide-binding assay system

DQA1*01:02-DQB1*06:02 cells were incubated with 0–500 μM biotinylated peptides and 100 μM non-biotinylated peptides at 37 °C. DQA1*01:02-DQB1*06:02 and DQA1*01:02-DQB1*06:04 cells were incubated with biotinylated and non-biotinylated insulin $B_{1\text{-}15}$ and insulin $B_{1\text{-}20}$ peptide at different concentrations. DQA1*01:02-DQB1*06:02 cells were incubated with various concentrations of biotinylated and non-biotinylated peptides after the cells were seeded in a 6-well plate for 4 h and 24 h, respectively. Cells were collected with or without trypsin, and signal intensities of binding peptides were quantified by flow cytometry (EPICS XL, Beckman Coulter Inc., California, USA).

2.3. Plate-based peptide-binding assay system

2.3.1. Peptide motif search

A couple of pockets in MHC molecules are responsible for the different preferences of MHC class II pockets for the side chains of different peptide anchor residues; these pockets consist of nine amino acids. The peptide anchor residues at positions P1, P4, P6, and P9 in the pockets of the MHC molecule interact with residues of peptides when the peptides are stretched in the binding groove. In this study, the peptide motif was designed based on a previously established binding motif (66). The motif model was obtained for HLA DQA1*01:02-DQB1*0602 peptide-binding pockets 1, 4, 6, and 9, as revealed by the binding of different lengths of insulin $B_{5\text{–}15}$

peptides in the grooves (66 64). In the HLA DQA1*01:02-DQB1*0602 peptide-binding motif model, P1 accommodates the amino acids A, N, D, C, E, Q, I, L, M, F, S, T, W, and Y and V; P4 accommodates A, N, Q, G, I, L, M, F, S, T, W, Y, and V; P6 accommodates L, I, V, A, S, P, and T; and P9 accommodates A, G, L, I, V, P, S, T, C, and M (66).

I designed 13- to 15-mer peptides containing amino-acid motifs P1, P4, P6, and P9 to detect potential antigen peptides for narcolepsy (38, 66). I searched for hypocretin peptides that contain the binding motifs P1: A, N, D, C, E, Q, I, L, M, F, S, T, W, Y, and V; P4: A, N, Q, G, I, L, M, F, S, T, W, Y, and V; P6: L, I, V, A, S, P, and T; and P9: A, G, L, I, V, P, S, T, C, and M. The designed hypocretin peptide was screened using TextWrangler software and custom-synthesized by GL Biochem Inc. The peptides hypocretin$_{1\text{-}13}$, hypocretin$_{14–25}$ hypocretin$_{26–39}$, hypocretin$_{45–55}$, hypocretin$_{57\text{-}69}$, hypocretin$_{79–89}$, hypocretin$_{89\text{-}99}$, hypocretin$_{79–89}$, and hypocretin$_{89\text{-}99}$ (Table 4) were dissolved in DMSO (Sigma–Aldrich Co. MO, USA) and used in the peptide-binding assay.

2.3.2. Cell lysate generation and protein quantification

DQA1*01:02-DQB1*06:02, DQA1*01:03-DQB1*06:01, DQA1 *01:03-DQB1*06:03, and DQA1*01:02-DQB1*06:04 cells were used for the plate-based peptide binding assay. Cells were seeded in 150-mm Petri dishes containing Dulbecco's Modified Eagle's medium supplemented with 6 μg/mL of puromycin and 2 mg/mL of G418; 10 mM sodium butyrate and 1 μM dexamethasone

were added 72 h before harvesting the cells. Approximately 4×10^7 cells were collected for the preparation of cell lysates.

Cells were lysed in PBS (pH 8.0) containing 0.5% (w/w) NP-40, 150 mM NaCl, 1× Complete Protease Inhibitor Cocktail (Roche Diagnostics GmbH, Mannheim, Germany), and 1 μL of Benzonase® nuclease (0.05 U/μL; Merck KGaA, Darmstadt, Germany). The mixture was incubated on ice for 1 h and centrifuged at 100 × *g* for 5 min at 4 °C. The supernatants were stored at −20 °C. Protein concentrations of the cell lysates were determined using the Protein DC assay (Bio-Rad Laboratories) according to the manufacturer's protocol, with bovine serum albumin (Sigma-Aldrich) as a standard.

2.3.3. Detection of binding of DQ6 protein on the nickel-coated plates

Lysates of NIH-DQA1*01:02-DQB1*06:02, NIH-DQA1*01:03-DQB1*06:01, NIH-DQA1*01:03-DQB1*06:03, and NIH-DQA1*01:02-DQB1*06:04 cells (0–60 μg) were applied to Pierce™ Nickel-Coated Plates (Thermo Fisher Scientific) with 120 mM NaCl and 0.4% (w/w) NP-40 in 1× PBS, immobilized in PBS (pH 7.0) containing 1× complete Protease Inhibitor Cocktail, and incubated at RT for 3 h. The plates were washed and incubated with anti-DR, DQ and DPβ mAb (clone WR18, 1 μg/ml), which react with DP, DQ, and DR beta chains, respectively, at RT for 60 min. The wells were washed 3 times with PBST, and the plates were incubated with 1/1000× HRP-conjugated goat anti-mouse IgG antibody (0.04 μg/mL; Santa Cruz Biotechnology Inc., Texas, USA) at RT for 60 min. Then, the plates were washed with PBST and incubated with the ECL™ Prime Western Blotting Reagent (GE Healthcare

Co., Uppsala, Sweden) at RT for 5 min. Chemiluminescence signals were detected and analyzed by using ChemiDoc XRS and Quantity One software.

2.3.4. Plate-based peptide-binding assay system

The plate-based peptide-binding assay system was developed to enable immobilization of the HLA-DR protein with the His-tag onto nickel ion-coated plates. This method was originally developed to allow type 1 diabetes risk- or protective-DR proteins to be immobilized on the plate surface in order to enable the screening of synthetic peptide ligands derived from the autogenic peptide ZnT8 (Dr. Cindy Chen, unpublished data). A reaction mixture that contained 60 μg of DQ protein lysates, PBS (pH 7.0) 4% (v/v) DMSO, 1× protease inhibitor cocktail, and 0.02% (w/v) n-dodecyl-β-D-maltoside in a final volume of 200 μL was applied to a Pierce™ nickel-coated plate for 3 h at RT. The plate was then washed using 200 μL of PBST. Subsequently, 200 μL of the peptide reaction mixture was added to the plate.

The peptide reaction mixture contained 0–150 μM biotinylated hypocretin peptides, 4% (v/v) DMSO, 1× protease inhibitor cocktail, and 0.02% (w/v) n-dodecyl-β-D-maltoside in PBS (pH 7.0). After incubation for 24 h at 37 °C, the peptide mixture was removed, and the plate was washed 3 times with 200 μL of PBST. Subsequently, 1/10,000× NeutrAvidin HRP conjugates (Thermo Fisher Scientific Inc., IL, USA; pH 7.0) were added, and the plates were incubated for 1 h at RT.

Fluorescence signals of the peptides were detected using a MTP-600F Fluorescence Microplate Reader (Corona Electrics, Ibaraki) and the QuantaBlu substrate (excitation and emission wavelengths of 415 nm and 360 nm, respectively). Chemiluminescence signals were detected using the ECL™ Prime Western Blotting

Detection Reagent and were analyzed using the ChemiDoc™ XRS and Quantity One software (GE Healthcare Co., Uppsala).

3. RESULTS

3. RESULTS

3.1. Establishment of mammalian cell lines that stably express HLA-DQ6 proteins

As shown in Figure 4, expression of the DQA1*01:02-DQB1*06:01, DQA1*01:03-DQB1*06:01, DQA1*01:02-DQB1*06:02, DQA1*01:03-DQB1*06:02, DQA1*01:02-DQB1*06:03, DQA1*01:03-DQB1*06:03, DQA1*01:02-DQB1*06:04, DQA1*01:03-DQB1*06:04, and DQA1-neo-DQB1-puro proteins was confirmed by flow cytometry (Figure 4). Several different approaches have been developed to produce recombinant proteins using peptide tags that do not interfere with the functioning of the fused protein (81). Expression of DQ proteins fused to His-tag or Strep-tag by NIH3T3 cells was confirmed by dot-blot analysis for DQA1*01:02-DQB1*06:02 (Figure 5).

3.2 Enhancement of cell-surface expression of DQ proteins

Sodium butyrate and dexamethasone are known to synergistically activate the retroviral long terminal repeat promoter to increase protein expression. In this study, the expression levels of DQ proteins stimulated by sodium butyrate and dexamethasone were quantified by flow cytometry. The optimal concentrations for expression were found to be 10 mM sodium butyrate and 1 μM dexamethasone. These conditions were established by Dr. Uchida (unpublished). The expression levels of DQ proteins were estimated at 48 h and 72 h. The DQ frequencies of flow cytometry before stimulation are indicated in black, and after stimulation are indicated in red. As shown in Figure 6, the expression level of DQ6 protein was higher at 48 h and 72 h after stimulation than in the absence of stimulation (Figure 6).

The peptide is situated within the pocket of the MHC class II molecule, and the pockets vary depending on the MHC allele. The antigen-presenting cells interact with the peptides and a denatured protein will form MHC class II-peptide complexes. In this study, I constructed DQA1*01:02-DQB1*06:01, DQA1*01:03-DQB1*06:01, DQA1*01:02-DQB1*06:02, DQA1*01:03-DQB1*06:02, DQA1*01:02-DQB1*06:03, DQA1*01:03-DQB1*06:03, DQA1*01:02-DQB1*06:04, and DQA1*01:03-DQB1*06:04 cell lines that express narcolepsy-associated HLA-DQ molecules and evaluated the binding of these molecules to hypocretin-derived peptides to elucidate the binding affinity of the MHC class II-peptide to the **pocket of the MHC class II molecule** to determine the autoimmune mechanism of narcolepsy. Subsequently, I determined the interactions between HLA combinations and variant hypocretin peptides by cell-based and plate-based methods.

3.3. Selection of avidins, streptavidin, and anti-biotin reagents for whole-cell HLA-peptide binding assays

Non-specific binding is a problem in different cell lines. The affinity of biotin for avidin, streptavidin, or anti-biotin antibody was detected by flow cytometry when different cell cultures were first incubated with the biotinylated peptides and avidin, streptavidin, or anti-biotin antibody. To determine the reagent with the lowest non-specific binding signal on the NIH3T3 cell surface, the non-specific binding affinity of various manufacturers' reagents on the NIH3T3 cell surface was examined. I attempted to analyze peptide binding through a cell-based binding assay using avidins, streptavidin, and anti-biotin labels and the biotinylated hypocretin and insulin peptides.

Lower non-specific binding signals on the cell surface will increase the signal intensity of the peptide binding assay. First, cells expressing MHC class II molecules were incubated with the biotinylated peptide. Second, bound peptides were quantitated by incubating the cells with the corresponding avidin, streptavidin, and anti-biotin reagents for signal amplification. Different avidins, streptavidin, and anti-biotin reagents bound to cell surface and caused non-specific binding signals, which interfered with the measurement, suggesting that detection in cells requires lower background signals. Finally, I selected avidin, streptavidin, or anti-biotin reagents with a lower non-specific binding signal on the NIH3T3 cell surface for the cell-based peptide binding assay. NIH3T3 cells were used to analyze non-specific binding of different avidins, streptavidin, and anti-biotin reagents on the cell surface. Peptide binding to HLA displayed on the cell surface was measured by flow cytometry.

As shown in Figure 7, nonspecific binding of ExtrAvidin®−R-Phycoerythrin (Sigma Aldrich), NeutrAvidin DyLight 550 (Thermo Scientific), StrepAvidin-PE (Invitrogen), PE-anti-Biotin (BioLegend), and PE-anti-Biotin (Rockland) to the cell surface of NIH-DQA1*01:02-DQB1*06:02 was observed. The nonspecific binding signals of NeutrAvidin DyLight 550 were weaker than those of the other reagents (Figure 8).

To confirm nonspecific binding of NeutrAvidin DyLight 550 at higher concentrations, NIH 3T3 cells were incubated with various concentrations of NeutrAvidin DyLight 550 (50 μM, 150 μM, and 500 μM). As shown in Figure 8, the

background signal was weak even at 500 μM (Figure 8). Therefore, NeutrAvidin DyLight 550 was used in all further experiments.

3.4. Cell-based HLA-peptide binding assays using insulin with or without trypsinization

Binding of biotinylated and competitor peptides under different conditions was analyzed for cell lines expressing HLA class II molecules (Figure 9). Insulin $B_{1\text{-}15}$ binds to DQA1*01:02-DQB1*06:02 and DQA1*01:02-DQB1*06:04 (66). I used insulin $B_{1\text{-}15}$ and insulin $B_{1\text{-}20}$ (which contains the insulin $B_{1\text{-}15}$ binding motif) as positive controls in this experiment.

Three different cell-based peptide-binding conditions were used to test the effects of (1) incubation time (4 and 24 h), (2) use of trypsin for the collection of cells, and (3) use of cell culture plates or plastic tubes for incubation with peptides (Figure 9). Bound insulin peptides were quantitated by incubating the cells with NeutrAvidin and estimating the fluorescence signals by flow cytometry. The flow cytometry histograms obtained in the previous experiment were used (Figure 9B). DR1-transfected and mock cells (untransfected DR cells) were incubated with the biotinylated $HA_{307\text{-}319}$ peptides (Figure 9B). The fluorescence signals of untransfected DR1 with $HA_{307\text{-}319}$ peptides and mock cells were used as negative controls in the cell-based peptide binding assay (82). Insulin $B_{1\text{-}15}$ and insulin $B_{1\text{-}20}$ bound to mock cells (untransfected DQ NIH3T3 cells) were used as negative controls in the cell-based peptide binding assay to compare the signals of DQA1*01:02-DQB1*06:02 and DQA1*01:02-DQB1*06:04 cells.

DQA1*01:02-DQB1*06:02 and DQA1*01:02-DQB1*06:04 cells were incubated with biotinylated and non-biotinylated peptides for 4 h in a 6-cm culture dish. After incubation, the cells were collected from the dish by trypsinization. As shown in Figure 10, signal intensities were similar for 100 μM biotinylated peptide with 50 μM competitor peptide (green) and for 100 μM competitor peptide alone (grey). The negative control (black) also exhibited similar signal intensities in DQA1*01:02-DQB1*06:02, DQA1*01:02-DQB1*06:04, and mock (negative control) cells (Figure 10). Insulin $B_{1–15}$ is known to bind to DQA1*01:02-DQB1*06:02 and DQA1*01:02-DQB1*06:04 (66). Under this condition, the difference between the DQA1*01:02-DQB1*06:04 and mock (negative control) cells was minimal. Accordingly, binding of insulin B_{1-15} to DQA1*01:02-DQB1*06:02 and DQA1*01:02-DQB1*06:04 cells was not detectable when trypsin was used for cell collection after incubation with insulin $B_{1–15}$ peptide.

Therefore, cells were collected in the absence of trypsin. Briefly, cells were incubated with the peptides for 4 h in a 6-cm culture dish. After incubation, cells were collected from the dish without trypsinization, and biotinylated peptide signals were measured by flow cytometry. As shown in Figure 11, the signal intensity of 500 μM biotinylated peptide (red) was higher than that of 50 μM biotinylated peptide (blue). However, nonspecific binding on mock cells was also detected.

The difference between the signal intensities of 500 μM biotinylated peptide (red) and 50 μM biotinylated peptide (blue) was more pronounced when the cells were collected by trypsinization rather than without trypsinization (Figure 11).

To increase the signal intensities on the DQA1*01:02-DQB1*06:02 and DQA1*01:02-DQB1*06:04 cell lines, the assay was also performed using a longer incubation time of 24 h. Cells were collected without trypsinization and were incubated with the peptides for 24 h in the culture plate. As shown in Figure 12, increased signal intensities were observed for 100 μM biotinylated peptide with 50 μM competitor peptide, 100 μM competitor peptide alone (green), and negative control (black; Figure 12). The signal intensities were largest at the highest peptide concentration. The signal intensities of 500 μM biotinylated peptide (red) and 100 μM biotinylated peptide with 50 μM competitor peptide (green) for DQA1*01:02-DQB1*06:02 cells were higher than those obtained for DQA1*01:02-DQB1*06:04 cells (Figure 12). However, increased nonspecific binding on mock cells was also detected.

These results indicate that trypsinization may reduce non-specific peptide binding to HLA; however, further modification of the assay is necessary to decrease non-specific binding on mock cells (Figures 11 and 12).

3.5. Effect of incubation time and incubation condition on whole-cell HLA-peptide binding assay

Next, I modified the protocol such that NIH3T3 cells were incubated with biotinylated peptide in 1.5-mL tubes. The cells were collected by trypsinization, incubated with biotinylated insulin $B_{1–20}$ peptides in the tubes, and shaken for 4 h to ensure peptide binding to the entire cell surface. As shown in Figure 13, the signal intensity of 500 μM biotinylated peptide alone (red) was higher than that in the presence

of 100 μM competitor peptide (grey) in DQA1*01:02-DQB1*06:02 and DQA1*01:02-DQB1*06:04 cells. However, the background signal intensities were high in mock cells (negative control), even at a concentration of 50 μM**.**

Next, the cells and peptides were incubated for 24 h. As shown in figure 14, extensive nonspecific binding of the peptide to the mock cell lines was observed. There were no differences in the signal intensities between DQA1*01:02-DQB1*06:02 or DQA1*01:02-DQB1*06:04 and mock cells. Therefore, the conditions tested in the experiment did not lead to reduced non-specific binding of the peptide or increased signal intensity for DQA1*01:02-DQB1*06:02 and DQA1*01:02-DQB1*06:04 cells.

As described in the previous sections, non-specific binding decreased when cells were collected without trypsinization and when the peptides were incubated with the cells in plates. Therefore, the assay protocol was modified appropriately.

For DQA1*01:02-DQB1*06:02 cells, signal intensities for biotinylated insulin $B_{1–20}$ peptides at 50 μM (blue), 250 μM (light green), and 500 μM (red) were higher than those for 100 μM biotinylated peptide with 50 μM competitor peptide (green) and 100 μM competitor peptide (grey). The signal intensity for insulin $B_{1–20}$ 100 μM biotinylated peptide with 50 μM competitor peptide (green) was low (Figure 15). However, under these conditions, the signal intensities of the mock cells were much higher than those of HLA-DQA1*01:02-DQB1*06:02 cells (Figures 14 and 15). The signal intensities of mock cells coated with 100 μM biotinylated peptide with 50 μM competitor peptide (green) were as high as those of 100 μM competitor peptide (grey) and negative control (black).

In summary, the cell-based peptide binding assay system was abandoned for two reasons, and a new finding was obtained for the cell-based peptide binding assay. The new finding was based on the plate-based peptide binding assay. First, even if in the experiment shown in Figure 15AB, the competitor peptide could decrease the signal accordingly, the cell-based peptide binding assay system exhibited low efficiency, especially for multiple MHC alleles, i.e., DQA1*01:02-DQB1*06:02 (risk haplotype), DQA1*01:03-DQB1*06:03 (resistant haplotype), DQA1*01:03-DQB1*06:03 (resistant haplotype), DQA1*01:02-DQB1*06:04 (neutral haplotype), and the negative control. Non-specific binding on the mock cell surface was found to be quite high using this method. The cell-based peptide binding assay system was designed for use in evaluating the binding of biotinylated peptides to HLA molecules displayed on murine fibroblast cells that were stably transduced with HLA-DQA1*01:02-DQB1*06:02 and HLA-DQA1*01:02-DQB1*06:04 alleles, and insulin peptides were used as indicator peptides. The signal intensities of the mock cell line with insulin $B_{1–15}$ and insulin $B_{1–20}$ were higher than that of untransfected DR1 with biotinylated $HA_{307-319}$ peptides (Figure 9B).

Second, although Epstein-Barr virus (EBV)-transformed cells have widely been used in cell-based peptide binding assays (82), these assays were unsuccessful in detecting specific binding of insulin B_{1-15} and insulin B_{1-20}, i.e., the positive control peptides, in NIH3T3 cells. In the cell-based peptide-binding assay, the assay system exhibited high non-specific binding under a variety of conditions.

The new finding in the cell-based peptide binding assay is that NeutrAvidin showed lower non-specific binding on the NIH3T3 cell surface (Figures 7 and 8). The reason for these findings is that NeutrAvidin has a neutral isoelectric point and lacks RYD sequences, but it retains the binding properties of native avidin observed in a previous study (38).

In contrast, as shown in Figure 9B, the cell-based peptide binding assay system used a lower peptide concentration, 50 μM, as the control. For insulin $B_{1\text{-}15}$ and insulin $B_{1\text{-}20}$, biotinylated peptide concentrations of 500 μM (red) (Figure 12) and 250 μM (light green) (red) (Figure 15) were used on NIH3T3 cells in the cell-based peptide binding assay under a variety of conditions. The cell-based peptide binding assay can thus be applied with NIH3T3 cells with high non-specific binding. Therefore, the cell-based assay system may be used for examination of single peptide binding affinity rather than screening of risk peptides.

The limitations of this method may be attributed to two possibilities. First, the use of NIH3T3 cells may have resulted in increased non-specific binding on the cell surface. Second, the use of insulin $B_{1–15}$ and insulin $B_{1–20}$ may be associated with non-specific binding on the NIH3T3 surface.

However, the plate-based peptide-binding assay showed higher discrimination for hypocretin$_{1\text{-}13}$ between the HLA-DQA1*01:02-DQB1*06:02 (susceptible) and mock cell lines. I used the plate-based peptide-binding assay to study the interaction between MHC protein and hypocretin peptide in further studies. Therefore, I selected a binding-assay system based on Ni^{2}+-coated plates for the subsequent experiments.

3.6. Preliminary binding assay for DQ proteins

First, to ensure immobilization of HLA class II proteins on Ni^{2+}-coated 96-well plates, various concentrations of lysates of DQ-expressing cells were incubated in Ni^{2+}-coated 96-well plates; lysates of DQA1*01:02-DQB1*06:02, DQA1*01:03-DQB1*06:01, DQA1*01:03-DQB1*06:01, and DQA1*01:02-DQB1 *06:04 expressing cells (total proteins, 60 μg; this concentration ensured that the same amount of HLA-DQ protein was bound on the plate) were immobilized on the Ni^{2+}-coated plates and saturated (Figures 16 and 17). Auto-antigen hypocretin peptide candidates were designed and synthesized on the basis of the full-length sequence of hypocretin (Figure 18) (66).

3.7. Assay for binding of insulin and hypocretin peptides to DQ6 proteins

In a previous study, the binding of hypocretin$_{1–13}$ to DQA1*01:02-DQB1*06:02 protein was characterized with regard to crystal structure and the binding of insulin B$_{1-15}$, insulin B$_{5-15}$, and insulin B$_{15-20}$ was evaluated in several types of cell-based binding assays (38, 66, 75, 77, 83). This is the first study evaluated the binding of hypocretin$_{1–13}$ and insulin B$_{1-15}$ to DQA1*01:03-DQB1*06:03 (resistant haplotype), DQA1*01:03-DQB1*06:03 (resistant haplotype), and DQA1*01:02-DQB1*06:04 (neutral haplotype) in the context of narcolepsy. In this study, eight new candidate peptides, i.e., hypocretin$_{14–25}$ hypocretin$_{26–39}$, hypocretin$_{45–55}$, hypocretin$_{57-69}$, hypocretin$_{79–89}$, hypocretin$_{89-99}$, hypocretin$_{79–89}$, and hypocretin$_{89-99}$, will be evaluated in the plate-based peptide binding assay. In particular, the binding intensity of the eight hypocretin candidate peptides to DQA1*01:03-DQB1*06:03 (resistant haplotype)

DQA1*01:03-DQB1*06:03 (resistant haplotype), and DQA1*01:02-DQB1*06:04 (neutral haplotype) will be addressed.

The intensity of the chemiluminescence signals for hypocretin$_{1–13}$ and insulin B$_{1-15}$ bound to DQ6 proteins on the Ni^{2+} plate was estimated using the ECL™ Reagent (Figure 9; each experiment was performed in duplicate). Chemiluminescence signals for hypocretin$_{1-13}$ and insulin B$_{1-15}$ peptides bound to DQA1*01:02-DQB1*06:02 proteins were measured. Biotinylated hypocretin$_{1-13}$ and insulin B$_{1-15}$ peptide were dissolved in 100% DMSO. Hypocretin$_{1–13}$ and insulin B$_{1–15}$ peptides (0–200 μM) were incubated with DQA1*01:02-DQB1*06:02 cell lysates (60 μg) and mock cell lysates (60 μg) at a pH of 7.0 at 37 °C for 24 h. The results revealed that hypocretin$_{1–13}$ peptide bound to DQA1*01:02-DQB1*06:02 protein, while insulin B$_{1–15}$ peptides bound non-specifically on both mock and DQA1*01:02-DQB1*06:02 cell lines.

3.7.1 Binding assay for hypocretin$_{1–13}$, hypocretin$_{14–26}$, and hypocretin$_{26-39}$

In a previous study, hypocretin$_{1–13}$ peptide was reported to bind to DQA1*01:02-DQB1*06:02 (38). The crystal structures of DQA1*01:02-DQB1*06:02 and hypocretin$_{1–13}$ have revealed that the molecular features underlying the presentation of hypocretin peptide on MHCs may play an important role in narcolepsy (38). For the plate-based peptide binding system (64, 66, 75, 83), different hypocretin peptides have been used previously to examine the epitopes of MHC. In the plate-based peptide binding system, hypocretin$_{1-13}$ bound to the DQA1*01:02-DQB1*06:02 product, indicating that the plate-based binding assay may

be applied to study the binding properties of other peptides. I chose hypocretin$_{1-13}$ and DQA1*01:02-DQB1*06:02 as positive controls.

In the preliminary experiment, binding of insulin $B_{1–15}$ and hypocretin$_{1–13}$ was examined by a plate-based peptide-binding assay. Hypocretin$_{1–13}$ peptide bound to DQA1*01:02-DQB1*06:02 protein, while insulin $B_{1–15}$ peptides showed non-specific binding on the mock cell line (negative control) (Figure 19). The insulin$_{1-15}$ and hypocretine$_{1-13}$ peptides were added and dissolved to DMSO. First, Insulin$_{1-15}$ looked insoluble in DMSO in eppendorf. In plate-based peptide binding assay, when the peptides can not be dissolved in DMSO, the wells showed as the bellowed wells of insulin1-15 with strange color and pattern. The wells of insulin$_{1-15}$ are inappropriate to calculate by cfu and rfu intensities by machine. The chemiluminescence signals were detected by seeing, ie.,visual inspection. Therefore, I used hypocretin$_{1–13}$ for further analysis.

Using hypocretin$_{1–13}$, a single-peptide binding assay was performed to optimize the binding conditions for HLA class II peptide and hypocretin$_{1–13}$. Cell lysates of DQA1*01:02-DQB1*06:02, DQA1*01:03-DQB1*06:01, DQA1*01:03-DQB1*06:01 and DQA1*01:02-DQB1* 06:04 cells (total proteins, 60 μg) were immobilized on a Ni^{2+}-coated plate. Biotinylated hypocretin$_{1–13}$ peptide was added, and the plates were incubated at 37 °C for 24 h. Unbound hypocretin$_{1–13}$ peptide was removed by washing to avoid non-specific binding.

In the plate-based peptide binding assay, increased signal intensities were observed with high concentrations of biotinylated hypocretin$_{1–13}$ peptide in wells that

contained DQA1*01:02-DQB1*06:02 and DQA1*01:03-DQB1*06:03 proteins. These results suggested that hypocretin$_{1–13}$ bound to DQA1*01:02-DQB1*06:02 (susceptible haplotype) and DQA1*01:03-DQB1*06:03 (resistant haplotype) more efficiently than to DQA1*01:03-DQB1*06:03 (resistant haplotype), DQA1*01:02-DQB1*06:04 (neutral haplotype), and the negative control (mock cells).

The results of the plate-based peptide binding assay system demonstrated that hypocretin$_{1–13}$ binds to HLA-DQA1*01:02-DQB1*06:02 (susceptible) and DQA1*01:03-DQB1*06:03 (protective) proteins; the experiment was repeated three times. This result suggested that the plate-based binding assay could be applied to analyze the binding of other hypocretin peptides to DQ proteins, using hypocretin$_{1–13}$ as the positive control.

In contrast, hypocretin$_{14–25}$ did not bind to any of the allele products tested in this study, as evidenced by the detection of non-specific binding on the mock cell line (negative control; Figure 20). As shown in Figure 21, hypocretin$_{26-39}$ exhibited strong binding to DQA1*01:03-DQB1*06:01, DQA1*01:02-DQB1*06:02, DQA1*01:03-DQB1*06:03, and DQA1*01:02-DQB1*06:04 proteins. This result was confirmed at lower concentrations of the peptide as well (Figure 21).

3.7.2 Binding assay for hypocretin$_{45–55}$, hypocretin$_{57–69}$, hypocretin$_{79–89}$, hypocretin$_{89–99}$, and hypocretin$_{116–128}$

As seen in Figure 22, hypocretin$_{57-69}$ bound to DQA1*01:03-DQB1*06:01, DQA1*01:02-DQB1*06:02, and DQA1*01:02-DQB1*06:04 proteins. Hypocretin$_{57-69}$

bound more strongly to DQA1*01:03-DQB1*06:01, DQA1*01:02-DQB1*06:02, and DQA1*01:02-DQB1*06:04 proteins than to DQA1*01:02-DQB1*06:03 protein.

Hypocretin$_{45–55}$, hypocretin$_{79–89}$, hypocretin$_{89–99}$ and hypocretin$_{116–128}$ harbor the DQA1*01:02-DQB1*06:02 binding motif; however, they did not bind to DQA1*01:02-DQB1*06:02. Hypocretin$_{14–25}$ bound to DQA1*01:02-DQB1*06:02 products, but showed non-specific binding to the mock cell line (negative control; Figure 19). Binding of hypocretin$_{45–55}$ to mock cells (negative control) may be attributed to the fact that hypocretin$_{45–55}$ is insoluble in DMSO and cannot conjugate with the MHC protein. Hypocretin$_{89–99}$ did not bind to DQA1*01:02-DQB1*06:02, possibly because it contains a methionine residue in the position corresponding to the tyrosine residue that usually competes with oxidizing free radicals to bind with proteins (Figures 23 and 24).

In a previous study, hypocretin$_{1–13}$ was shown to bind to the DQA1*01:02-DQB1*06:02 product, and the hypocretin$_{53-67}$-DQA1*01:02-DQB1*06:02 complex was recognized by T cells derived from narcoleptic patients (38, 84 85). In this study, hypocretin$_{57-68}$, which contains the same binding motif as hypocretin$_{53-67}$, bound to DQA1*01:02-DQB1*06:02. Hypocretin$_{1-13}$ also bound to the DQA1*01:02-DQB1*06:02 product. These results demonstrate that the plate-based binding assay may be applied to study the binding of other peptides as well.

To the best of my knowledge, this is the first study to standardize a systematic binding assay for prepro-hypocretin-derived peptides with risk- and protective-

HLA-DQ proteins associated with narcolepsy. I generated the new finding that hypocretin$_{1–13}$, hypocretin$_{26–39}$, and hypocretin$_{57-69}$ bind to DQA1*01:02-DQB1*06:02; hypocretin$_{1–13}$ and hypocretin$_{26–39}$ bind to DQA1*01:03-DQB1*06:03; hypocretin$_{26–39}$ and hypocretin$_{57-69}$ bind to DQA1*01:02-DQB1*06:04; and hypocretin$_{26–39}$, and hypocretin$_{57-69}$ bind to DQA1*01:03-DQB1*06:01. Eight new candidate peptides, hypocretin$_{14–25}$ hypocretin$_{26–39}$, hypocretin$_{45–55}$, hypocretin$_{57-69}$, hypocretin$_{79–89}$, hypocretin$_{89-99}$, hypocretin$_{79–89}$, and hypocretin$_{89-99}$, and three different HLA haplotype proteins, DQA1*01:03-DQB1*06:01, DQA1*01:03-DQB1*06:03, and DQA1*01:02-DQB1*06:04, were examined in this study (Table 4). The plate-based peptide assay system exhibited higher sensitivity and specificity than the cell-based assay methods. This assay system can be applied to screen auto-antigens against HLA-DQ6 proteins in the NIH3T3 cell expression system

4. DISCUSSION

4. Discussion

Whether narcolepsy is an autoimmune disorder is a compelling question. Hypocretin deficiency has been detected in sporadic HLA-*DQB1*06:02*-positive adolescent-onset narcolepsy cases (38). It has been hypothesized that autoimmune-triggered hypocretin loss is a central pathogenic factor for narcolepsy (86, 87), and that the susceptible *HLA-DQA1*01:02-DQB1*06:02* haplotype product might recognize hypocretin peptide or other antigens and mediate the autoimmune responses. However, the interactions between hypocretin-derived peptides and different HLA-DQ proteins specifically associated with narcolepsy have not been discussed previously.

In previous studies, Epstein-Barr virus (EBV)-transformed cells have been widely used (82). I selected NeutrAvidin for the cell-based peptide binding assay with low non-specific binding on the cell surface (Figures 7 and 8). However, it was unsuccessful in detecting specific binding of the positive control peptides, insulin $B_{1\text{-}15}$ and insulin $B_{1\text{-}20}$, in NIH3T3 cells, and the cell-based peptide binding assay system exhibited high non-specific binding under a variety of conditions. The plate-based peptide-binding assay showed better discrimination of hypocretin$_{1\text{-}13}$ binding between the HLA-DQA1*01:02-DQB1*06:02 (susceptible) and mock cell lines.

The binding signals for binding of hypocretin$_{1\text{-}13}$ to the DQA1*01:02-DQB1*06:02 product appeared stronger than those for the binding of hypocretin$_{1\text{-}13}$ to the DQA1*01:03-DQB1*06:01 product. The peptide binding assay showed binding of hypocretin$_{1\text{-}13}$ not only to HLA-DQA1*01:02-DQB1*06:02

(susceptible) but also to DQA1*01:03-DQB1*06:01 (resistant) and DQA1*01:03-DQB1*06:03 (resistant). This result first suggests the possibility of a pathogenic mechanism for narcolepsy involving not only HLA-DQA1*01:02-DQB1*06:02 (susceptible) but also DQA1*01:03-DQB1*06:01 (resistant), and DQA1*01:03-DQB1*06:03 (resistant). Second, the amino acid binding intensity will affect the different strengths of peptide binding.

These results first suggest that DQA1*01:03-DQB1*06:01 (resistant) and DQA1*01:03-DQB1*06:03 (resistant) might be associated with the pathogenic mechanism of narcolepsy. DQA1*01:03-DQB1*06:01 (resistant) and DQA1*01:03-DQB1*06:03 (resistant) recognize hypocretin peptides and therefore mediate the autoimmune response. This new finding is valuable for elucidating the mechanism of narcolepsy. These results suggest a relationship between the eight new hypocretin candidate peptides and narcolepsy-associated DQ alleles.

In the binding of hypocretin$_{1\text{-}13}$, valine was found to be accommodated in the P6 binding pocket in the crystal structure of DQA1*01:02-DQB1*06:02 in a previous study (38). DQA1*01:02-DQB1*06:02 and DQA1*01:03-DQB1*06:03 differ only at Phe9β in DQB1*06:02, Tyr9β in DQB1*06:03, Tyr30β in DQB1*06:02, and His30β in DQB1*06:03. 9β and 30β are involved in accommodating P6 in the binding pocket (Table 1). In this study, because the signal intensities of hypocretin$_{1\text{-}13}$ binding to DQA1*01:03-DQB1*06:03 protein appeared to be as strong as those of

DQA1*01:02-DQB1*06:02, differences at 9β and 30β may not affect the accommodation of P6 valine (Figure 20, Table 1).

DQA1*01:02-DQB1*06:02 and DQA1*01:03-DQB1*06:03 differ only at Phe9β in DQB1*06:02, Tyr9β in DQB1*06:03, Tyr30β in DQB1*06:02, and His30β in in DQB1*06:03. 9β and 30β are involved in accommodating P6 in the binding pocket. Because the signal intensities of hypocretin$_{1\text{-}13}$ binding to DQA1*01:03-DQB1*06:03 protein appeared to be as strong as those of DQA1*01:02-DQB1*06:02, differences at 9β and 30β may not affect the accommodation of P6 valine (Figure 20, Table 1).

The DQB1*06:01 and DQB1*06:02 proteins have different residues at P4 and P9; different residues occur at 13β and 26β on the P4 pocket and at 37β and 38β on the P9 pocket (Ala13β, Tyr26β, and Val38β in DQB1*06:01; Gly13β, Leu26β, and Ala38β in DQB1*06:02). I could not identify which of these residues are responsible for the particularly stronger binding of hypocretin$_{1\text{-}13}$ with DQA1*01:02-DQB1*06:02 than with DQA1*01:03-DQB1*06:01 (Figure 20, Table 1).

The DQB1*06:02, DQB1*06:03, and DQB1*06:04 proteins have different amino acid sequences at P6 and P9. DQA1*01:02-DQB1*06:02 and DQA1*01:03-DQB1*06:03 differ at 9β and 30β, which are involved in accommodating P6. DQA1*01:02-DQB1*06:02 and DQA1*01:02-DQB1*06:04 differ at Phe9β in DQB1*06:02, Tyr9β in DQB1*06:04, Tyr30β in DQB1*06:02, His30β in in DQB1*06:04, Asn57β in DQB1*06:02, and Val57β in DQB1*06:04. 9β and 30β are involved in accommodating P6 while 57β is involved in accommodating P9 (Table 1).

The MHC class II molecule has an open binding groove containing the peptide-binding segment, and peptide residues are bound in the peptide binding groove. The hypocretin peptide side chains at positions 3, 6, 8, and 11 occupy HLA DQ peptide-binding pockets 1, 4, 6, and 9, whereas the remaining peptide residues are outside the groove. The difference between DQA1*01:02 and DQA1*01:03 may be attributed to differences in the amino acids outside the groove. The difference in the relative fluorescent intensities for the binding of hypocretin$_{1\text{-}13}$ to DQA1*01:03-DQB1*06:03 and DQA1*01:02-DQB1*06:02 may thus represent differences in the binding strength of DQA1*01:03 or DQA1*01:02-DQB1*06:02 (Table 1).

The binding of hypocretin$_{26–39}$ with the DQA1*01:03-DQB1*06:03 product was stronger than that with DQA1*01:03-DQB1*06:01, DQA1*01:02-DQB1*06:02, and DQA1*01:02-DQB1* 06:04, as evidenced by the relative fluorescence units, and this was a new finding (Figure 21). DQA1*01:03-DQB1*06:03 contains Tyr9β and Asp57β, which provide a net positive charge and obstruct binding to hypocretin$_{26–39}$, compared to Phe9β in DQB1*06:02 and Val57β in DQB1*06:04. DQA1*01:02-DQB1*06:02, DQA1*01:03-DQB1*06:03, and DQA1*01:02-DQB1*06:04 differ at Tyr25α in DQA1*01:02, Phe25α in DQA1*01:03, Arg41α in DQA1*01:02, and Lys41α in DQA1*01:03 (Figure 21, Table 1).

For the binding of hypocretin$_{57–69,}$ the binding of the hypocretin peptide segment to DQA1*01:02-DQB1*06:02 and DQA1*01:03 -DQB1*06:01 was stronger than that to DQA1*01:03-DQB1*06:03 (Figure 22). DQB1*06:02 and DQB1*06:03 encode

identical residues at P4 and P9, and these residues are different from those in DQB1*06:01 (Table 1). However, hypocrein$_{57\text{-}69}$ binds to DQB1*06:01 and DQB1*06:02, suggesting that P6 plays a role in epitope selection.

Previous studies have revealed that the preferred amino acids of DQB1*06:02 in P6 are large aliphatic amino acids, while those in P9 are smaller aliphatic and hydroxyl amino acids (66). DQB1*06:01 encodes Asp37β and Val38β in P9, which binds to Leu64 in hypocretin$_{57–69}$. DQB1*06:02 encodes Phe9β, Tyr30β, and Gln66β, and DQB1*06:03 encodes Tyr9β, His30β, and Gln66β on P6, which binds to Ile62 in hypocretin$_{57–69}$ (Table 1). One possible reason for the weak binding of hypocretin$_{57–69}$ to DQB1*06:03 compared with other alleles may be the presence of His30β, which provides only one positive charge in P6. The other anchor residues of P4 and P9 are identical in DQB1*06:02, DQB1*06:03, and DQB1*06:04 (Table 1).

Additionally, the differences in binding affinity of DQB1*06:01, DQB1*06:02, and DQB1*06:04 to hypocretin$_{57–69}$ may be explained by the presence of 67β, 70β, 86β, and 87β, as the remaining hypocretin peptide residues are not located in the MHC class II binding pocket (Table 1).

One possible role for the binding of hypocretin$_{26–39}$ to DQA1*01:03-DQB1*06:03 and HLA-DQA1*01:03-DQB1*06:01 or hypocretin$_{57–69}$ to HLA-DQA1*01:03-DQB1*06:01 is that hypocretin$_{26\text{-}39}$ or hypocretin$_{57–69}$ peptides trigger an immune protection mechanism in which T-helper cells stimulate B-cells to produce antibodies. Hypocretin$_{26\text{-}39}$ or hypocretin$_{57–69}$ peptides are released into the

synaptic cleft, where they bind to a protective protein and trigger an immune response or protection mechanism.

This effect may be caused by T-cell tolerance. T cells cause enormous damage when they are not appropriately directed to recognizing pathogen fragments of surface molecules on host cells. This represents a potential threat to tolerance to self. Recent mechanistic studies on T-cell tolerance have provided insights that may aid the development of therapeutic strategies to treat autoimmune disease (88). Distinct αβ T cell receptors with random specificity to high-affinity self-peptide-MHC overcome failure of T-cell tolerance and autoimmune reactions.

T-cell tolerance may also explain why hypocretin$_{57–69}$ binding to DQA1*01:02-DQB1*06:02 process is not 100% efficient. The weak binding of hypocretin$_{57–69}$ to the HLA-DQ risk allele protein products indicates that weaker stimulation signals may evade major immune responses in the thymus and present self-peptides to T cells in the hypothalamus. The strong binding signals of hypocretin to DQA1*01:02-DQB1*06:02 may be stimulated initially. However, weaker binding of hypocretin$_{57–69}$ to DQA1*01:02-DQB1*06:02 may be retained and stimulated at a later point under environmental conditions. Binding signals of different strengths for the binding of hypocretin to DQA1*01:02-DQB1*06:02 or other alleles might be stimulated at different moments. These differences in the binding signals of hypocretin to DQA1*01:02-DQB1*06:02 may play a role in H1N1 infection, resulting in the destruction of hypocretin neurons.

Narcolepsy with hypocretin deficiency is associated with *HLA* and T cell receptors, and an autoimmune mechanism may target unique peptides in the cell. A recent study on influenza H1N1-infection and H1N1-vaccination has suggested that processes such as molecular mimicry are crucial for disease development. Because the loss of hypocretin-producing neurons causes narcolepsy with cataplexy, I examined various hypocretin peptides to identify specific peptides that bind to the risk or protective DQ isoforms associated with narcolepsy. My findings suggest that narcolepsy is an autoimmune disease.

In this study, the results of the plate-based peptide-binding assay were reproducible. Screening a large number of candidate peptides for diverse HLA allele products might facilitate the detection of potential epitopes such as TRIB2 or NARP (89, 90). The results described in this thesis need to be verified by using T cells from narcoleptic patients in future studies. The results provide new insights into the epitopes and molecular mechanisms underlying narcolepsy.

5. FIGURES & TABLES

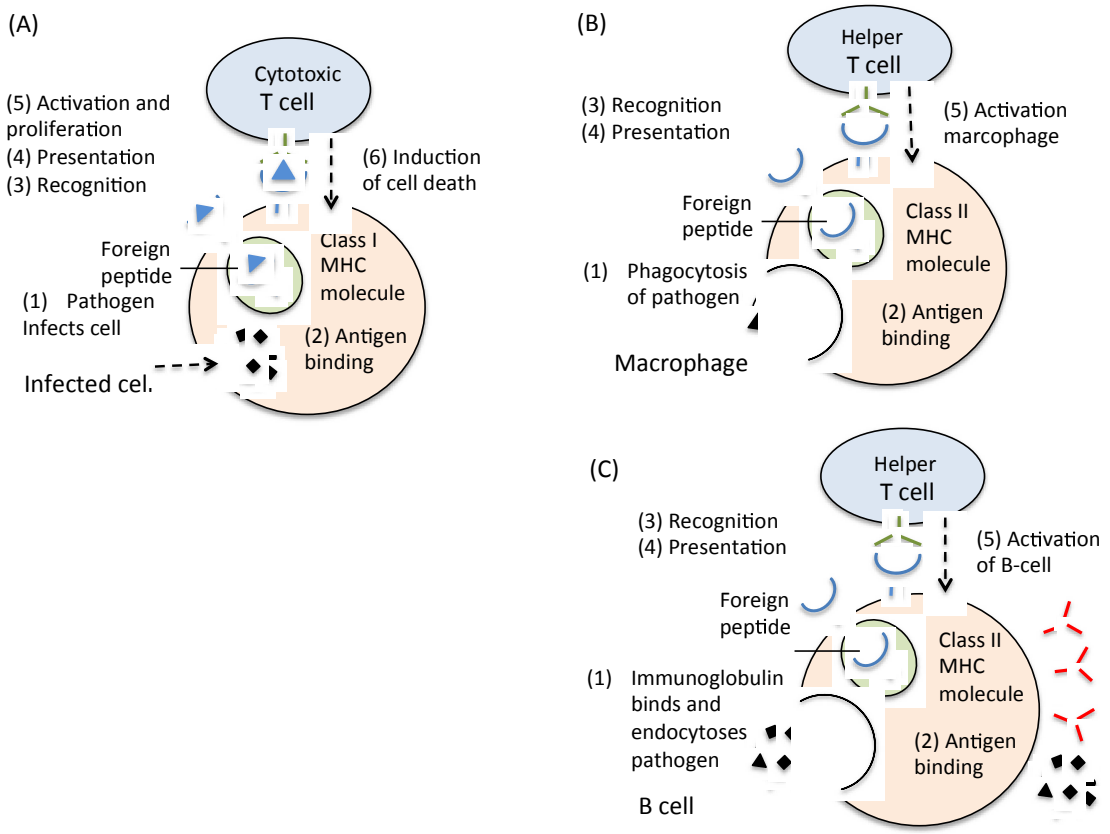

Figure 1. Antigen presentation by MHC class I and II molecules to T cells. Cytotoxic T cells bind to foreign peptides in association with class I MHC proteins, whereas helper T cells bind to foreign peptides in association with class II MHC proteins. Cytotoxic T cells and helper T cells recognize the peptide-MHC complexes on the surface of an antigen-presenting cell or a target cell ([91]). (A) The peptide presented by MHC class I molecules on the cell surface interacts with CD8 (+) cells. (B) MHC class II presents processed antigens, which are derived primarily from exogenous sources, to CD4 (+) T-lymphocytes. T cells recognize the MHC class II–peptide complex on the surface of antigen-presenting cells. (C) MHC class II–peptide complexes on B lymphocytes initiate the antigen-specific immune response.

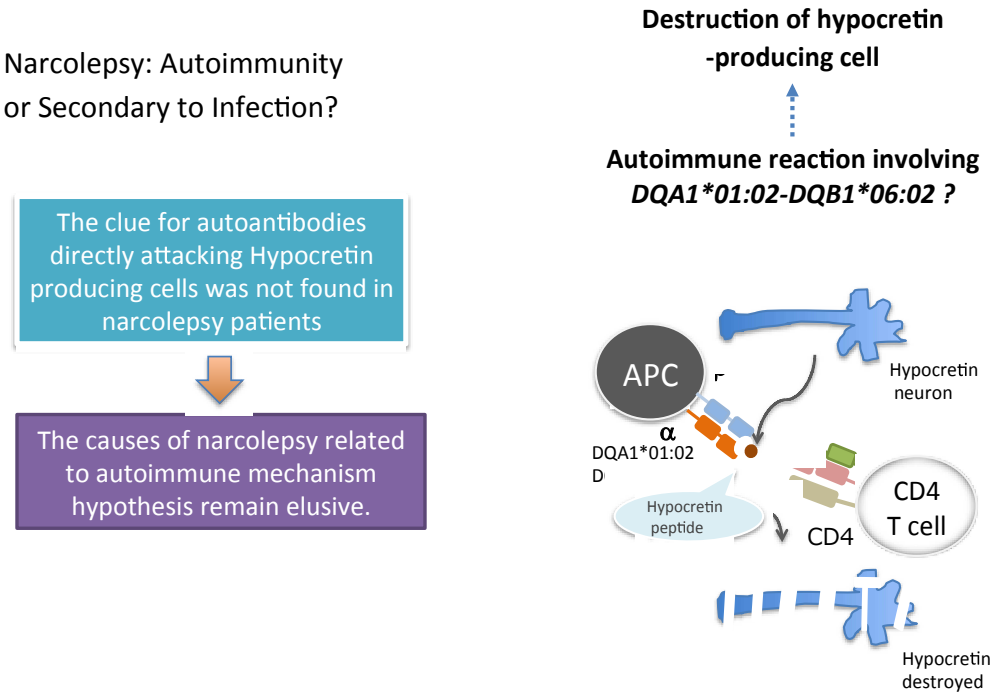

Figure 2. Hypothetical mechanism of narcolepsy

Whether narcolepsy is an autoimmune disorder is a compelling question. Autoantibodies that directly attack hypocretin-producing cells have not been detected in narcolepsy patients. It has been hypothesized that hypocretin-producing cells are destroyed in narcoleptic brain cells because hypocretin peptides specifically expressed in hypocretin-producing cells in the hypothalamus are presented by HLA-DQA1*01:02-DQB1*06:02, which is recognized by T cells, resulting in an autoimmune response.

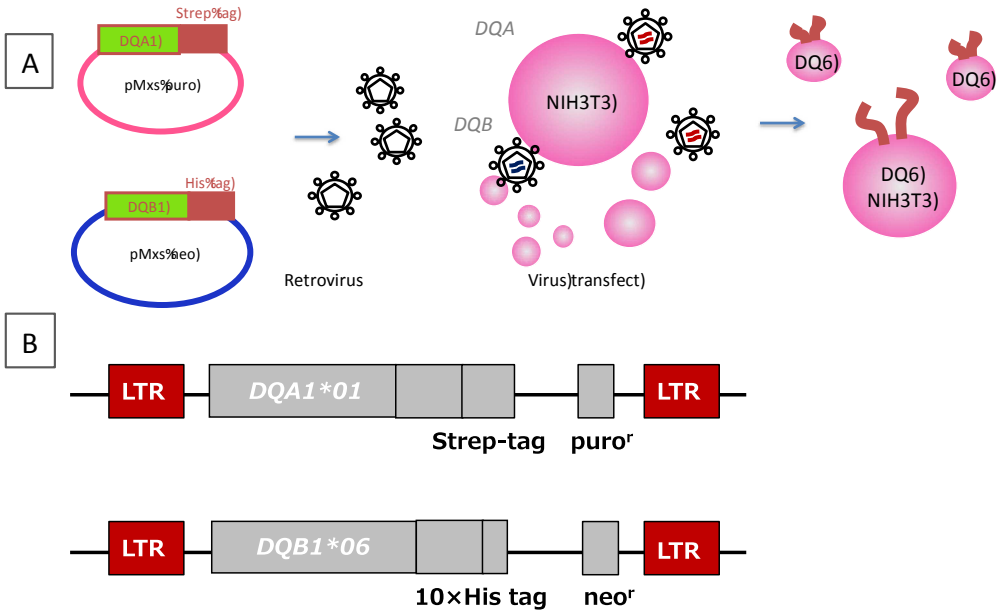

Figure 3. Construction of stable DQ06 cells

(A) *DQA1*01* cDNA, which was fused with Strep-tag II, and *DQB1*06* cDNA, which was fused with a 6× histidine tag (His-tag), were inserted into pMXs-puro and pMXs-neo, respectively. Recombinant proteins were expressed in NIH3T3 cells, and the protein expression levels were enhanced. (B) pMXs-puro/*DQA1*01* and pMXs-neo/*DQB1*06* vectors were designed with long terminal repeat (LTR) sequences. Recombinant DQ protein was expressed under the retrovirus LTR promoter in NIH3T3 cells. Sodium butyrate and dexamethasone increase DQ protein transcription from the LTR present in NIH3T3 cells.

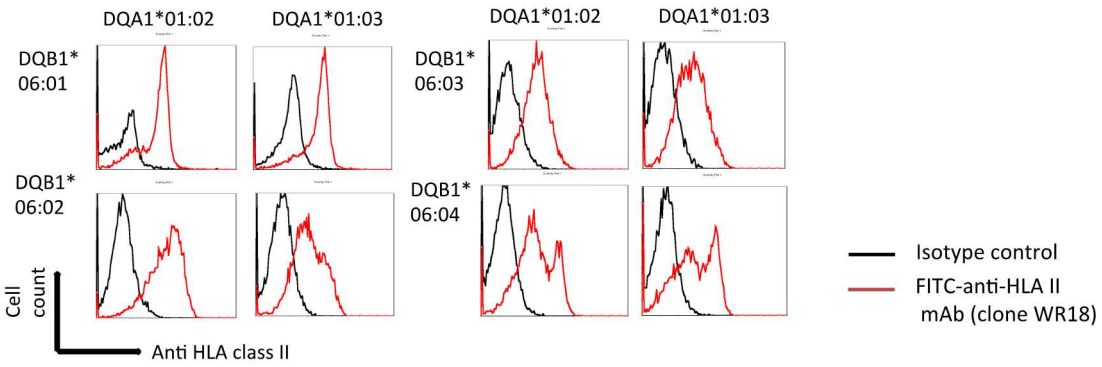

Figure 4. Stable expression of DQ*06 proteins in a mammalian cell line

DQ*06-expressing NIH3T3 cells were incubated with (FITC)-conjugated anti-HLA-DR, -DQ, and -DPβ monoclonal antibodies (mAb; clone WR18; Morphosys A.G., Munich, Germany) at 4 °C for 20 min. Fluorescence intensities were measured and analyzed by flow cytometry (EPICS XL, Beckman Coulter Inc., California, USA). The expression of DQA1*01:02-DQB1*06:01, DQA1*01:03-DQB1*06:01, DQA1*01:02-DQB1 *06:02, DQA1*01:03-DQB1*06:02, DQA1*01:02-DQB1*06:03, DQA1*01:03 -DQB1*06:03, DQA1*01:02-DQB1*06:04, and DQA1*01:03-DQB1 *06:04 proteins was confirmed by flow cytometry.

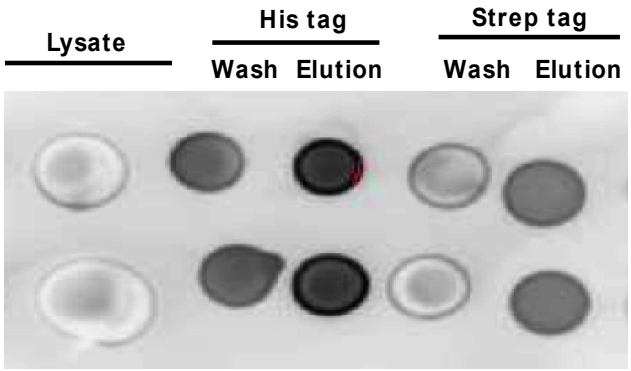

Figure 5. Dot-blot analysis of the DQA1*01:02-DQB1*06:02 protein

NIH-DQ0602 protein expression was confirmed by dot-blot analysis. Five-microliters (each) of the cell lysates, wash samples, and elutes of the His- and Strep-tagged DQA1*01:02-DQB1*06:02 proteins were spotted on a nitrocellulose membrane (GE Healthcare Co., Uppsala, Sweden). DQA1*01:02-DQB1*06:02 was detected using anti-his-tag mAb. The top and bottom spots correspond to the doubling test.

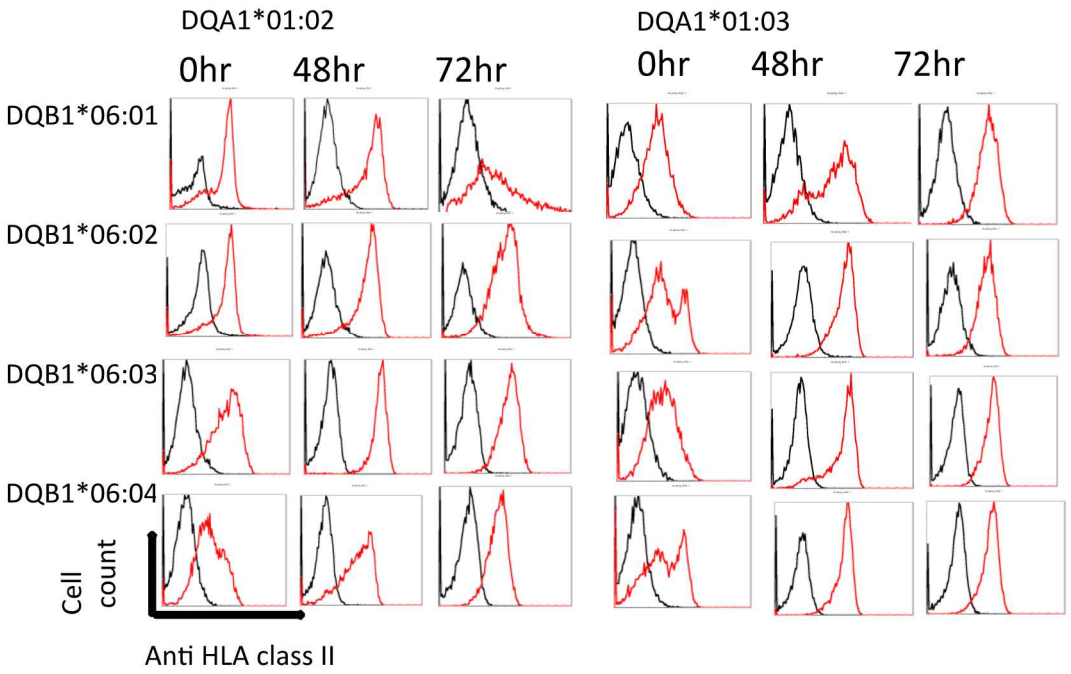

Figure 6. Enhancement of DQ6 protein expression

The culture time for MHC class II protein expression in NIH3T3 cells was optimized by Dr. Yuki Uchida in our laboratory. NIH-DQA1*0102-DQB1*0602 (susceptible haplotype), NIH-DQA1*0103- DQB1*0601 (resistant haplotype), NIH-DQA1*0103-DQB1*0603 (resistant haplotype), and NIH-DQA1*0102-DQB1*0604 (neutral haplotype) cells were incubated with 10 mM sodium butyrate and 1 μM dexamethasone for 48 h and 72 h. NIH-DQA1*0102-DQB1*0602 (susceptible haplotype), NIH-DQA1*0103-DQB1*0601 (resistant haplotype), NIH-DQA1*0103-DQB1*0603 (resistant haplotype), and NIH-DQA1*0102-DQB1*0604 (neutral haplotype) cells were incubated with FITC-conjugated anti-HLA-DR, -DQ, and -DPβ mAbs (clone WR18; Morphosys A.G., Munich, Germany) and isotypic control IgG2a-FITC (Beckman Coulter, Inc., US) at 4 °C for 20 min. Fluorescence intensities were measured and analyzed by flow cytometry (EPICS XL, Beckman Coulter Inc., California, USA).

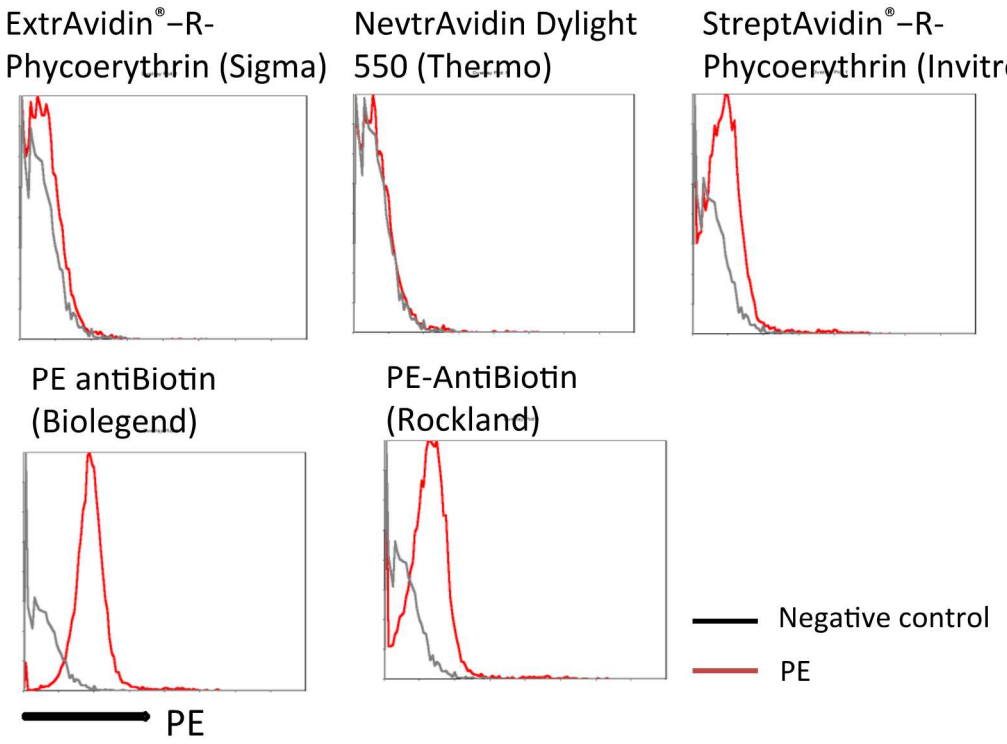

Figure 7. Analysis of non-specific binding to the NIH3T3 cell surface

Flow cytometric analysis of avidin binding to the NIH3T3 cell surface. The Phycoerythrin (PE), red protein-pigment complex from the light-harvesting is designed for avidin and anti-biotin in this study. The nonspecific binding of avidins with Phycoerythrin (PE) labeled, obtained from various manufacturers, on the NIH3T3 cell surface was examined. The reagents, ExtrAvidin®–R-Phycoerythrin (E4011, Sigma Aldrich), NeutrAvidin DyLight 550 (84606, Thermo Scientific), StrepAvidin-PE (S866, Invitrogen), PE-anti-Biotin (409004, BioLegend), and PE-anti-Biotin (600-108-098, Rockland), were in concentration: 0.01 μg/μL and incubated with 5×10^5 NIH3T3 cells for 24 h at 37 °C (78-80). Signals for the avidins were measured by flow cytometry.

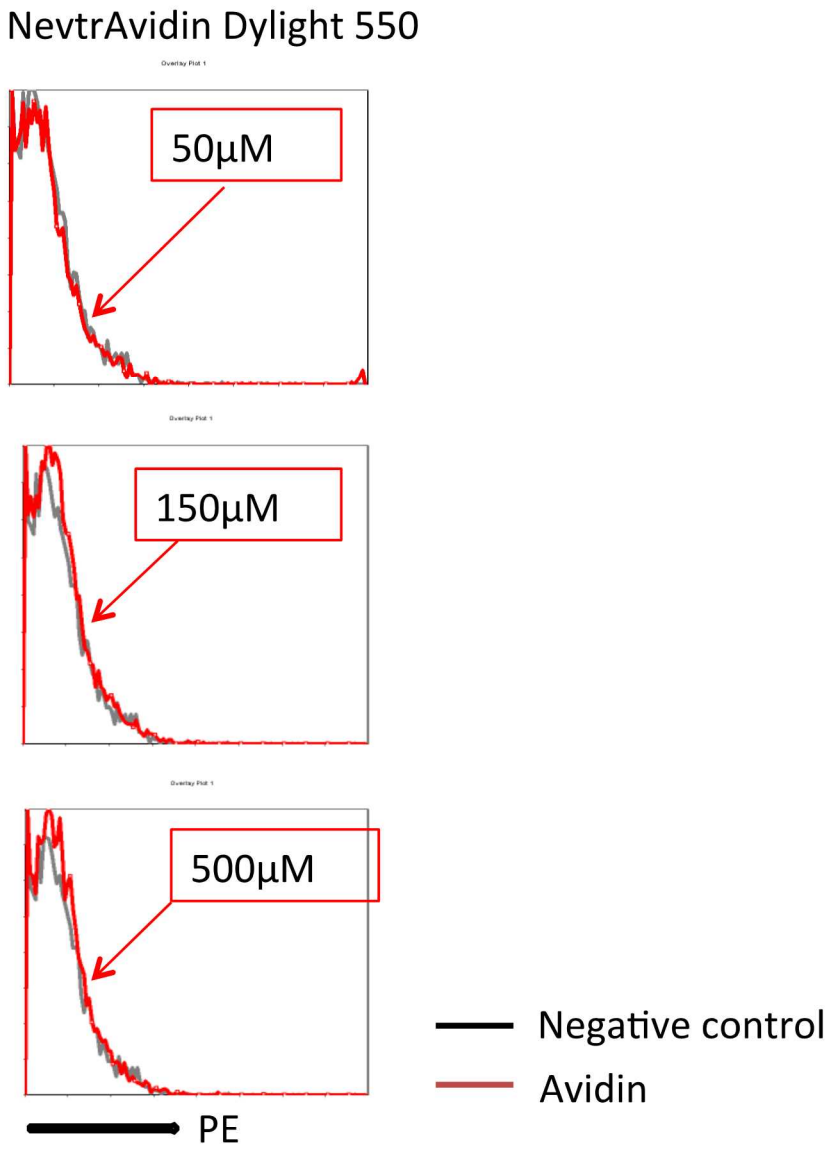

Figure 8. Negligible nonspecific binding of NeutrAvidin to the surface of NIH3T3 cells

The cell-surface binding of NeutrAvidin DyLight 550 was measured at 50 µM, 150 µM, and 500 µM (excitation and emission wavelengths of 562 nm and 576 nm, respectively). NIH3T3 cells were incubated with different concentrations of NeutrAvidin DyLight 550. Fluorescence intensities were measured and analyzed by flow cytometry (EPICS XL, Beckman Coulter Inc., California, USA).

(A)

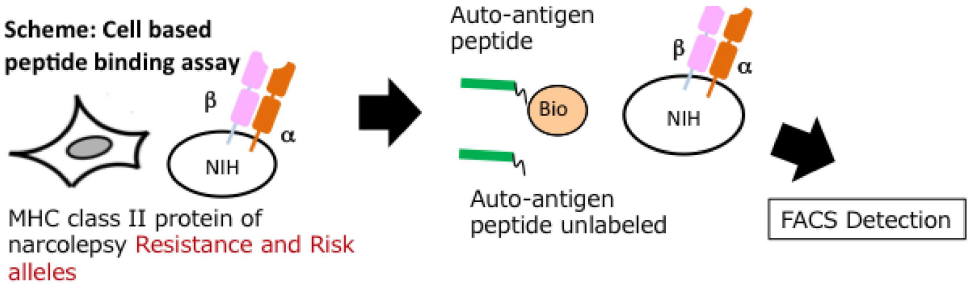

(B)

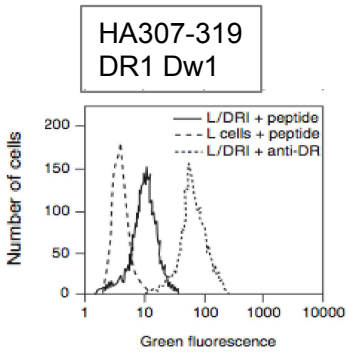

Figure 9. Cell-based peptide binding assay

(A) A cell-based peptide binding assay system was tested using murine fibroblast cells that were stably transduced with the HLA-DQA1*01:02-DQB1*06:02 and HLA-DQA1*01:02-DQB1*06:04 alleles by using retrovirus vectors; insulin peptides were used as indicators. (B) In the previous assay described for HLA-DR, biotinylated peptides were allowed to bind to MHC class II molecules on the surface of Epstein-Barr virus-transformed B cells (EBV–B cells). Representative examples of flow cytometry histograms showing binding of $HA_{307-319}$ peptide to DR1 molecules on whole cells. Cells were incubated with and without biotinylated $HA_{307-319}$ peptide and stained with streptavidin-FITC, or anti-DR/DP mAb and goat-anti-mouse-Ig-FITC (Adapted from references 82, 92).

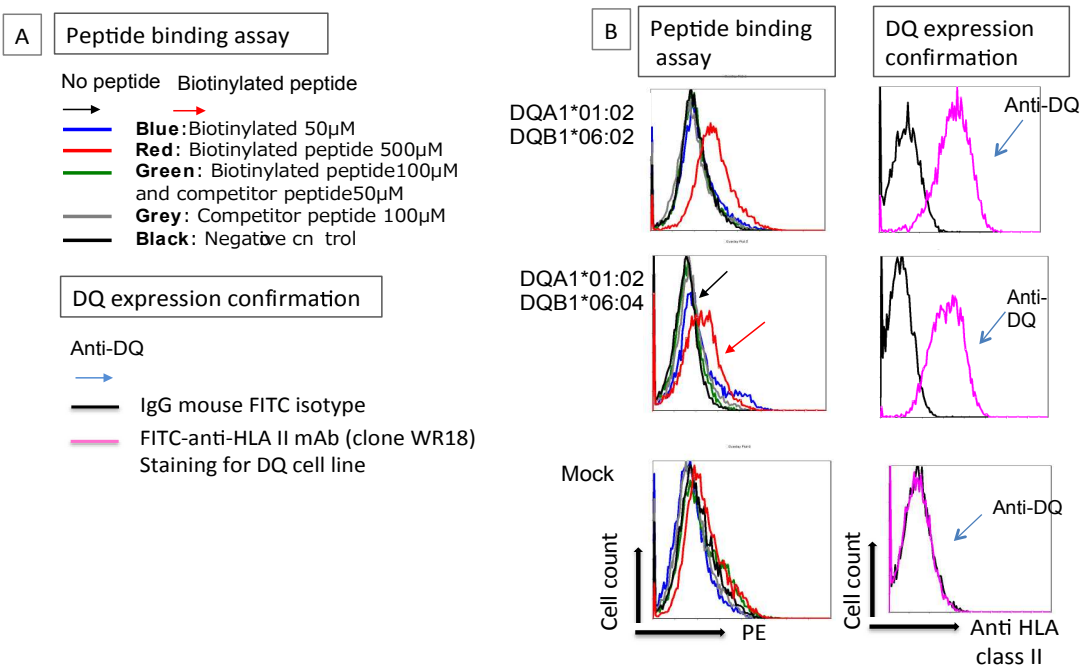

Figure 10. Binding of insulin $B_{1–15}$ to the DQ6 proteins

(A) Insulin B_{1-15} showed strong binding to HLA-DQA1*01:02-DQB1*06:02 and HLA-DQA1*01:02-DQB1*06:04 proteins, as reported previously (66, 75). Different concentrations of human insulin $B_{1–15}$ peptide (0–500 μM) were incubated with DQA1*01:02-DQB1*06:02, DQA1*01:02-DQB1*06:04, and mock cells in a 6-well plate at 37 °C for 4 h. After incubation, cells were collected from the dish by trypsinization. Biotinylated insulin $B_{1–15}$ peptide was dissolved in 95% DMSO and 5% β-mercaptoethanol. DQ*06 protein-expressing NIH3T3 cells were incubated with FITC-conjugated anti-HLA-DR, -DQ, and -DPβ -mAbs (clone WR18; Morphosys A.G., Munich, Germany) at 4 °C for 20 min. (B) Flow cytometry signals for insulin $B_{1–15}$ peptide bound to DQA1*01:02-DQB1*06:02, DQA1*01:02-DQB1*06:04, and mock cells. Expression of DQ*06 proteins in NIH3T3 cells was confirmed and analyzed by flow cytometry (EPICS XL, Beckman Coulter Inc., California, USA).

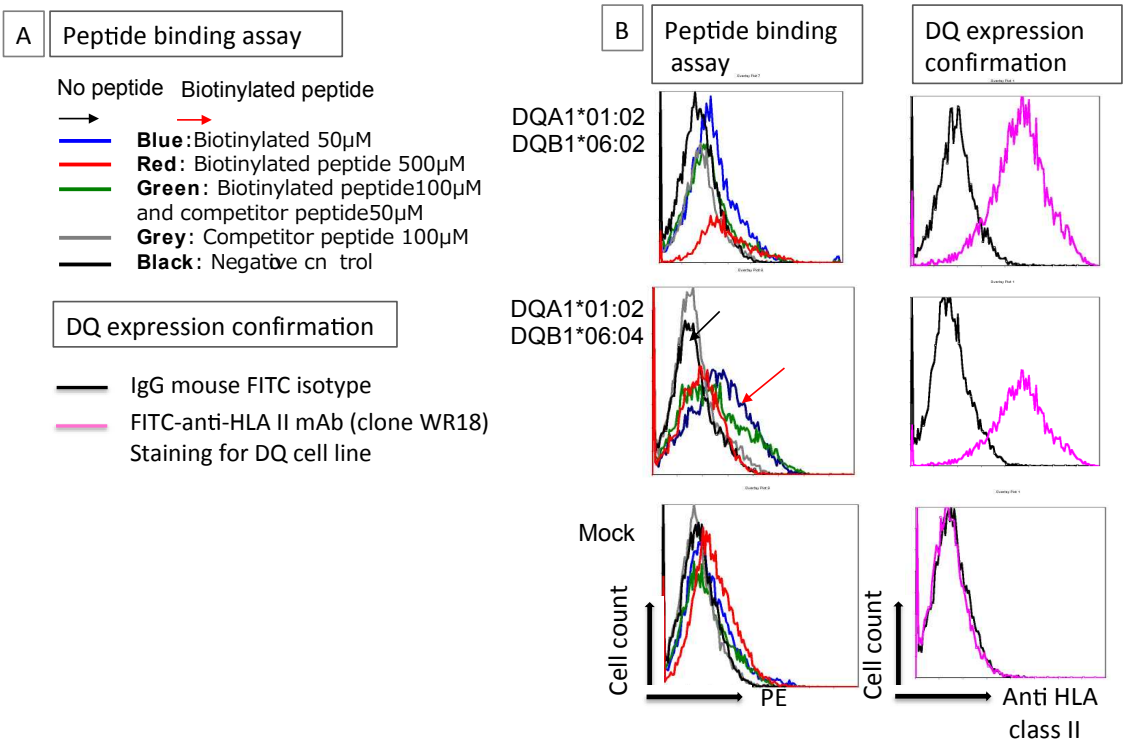

Figure 11. Binding of insulin $B_{1–15}$ to the DQ6 proteins in the absence of trypsinization

(A) DQA1*01:02-DQB1*06:02, DQA1*01:02-DQB1*06:04, and mock cells were incubated with insulin $B_{1–15}$ peptide (0–500 μM) at 37 °C for 4 h. Then, the cells were collected without trypsinization. Biotinylated insulin $B_{1–15}$ peptide was dissolved in 95% DMSO and 5% β-mercaptoethanol. DQ*06 protein-expressing NIH3T3 cells were incubated with FITC-conjugated anti-HLA-DR, -DQ, and -DPβ mAbs (clone WR18; Morphosys A.G., Munich, Germany) at 4 °C for 20 min. (B) Flow cytometry signals for insulin $B_{1–15}$ peptide bound to DQ*06 protein-expressing NIH3T3 cells were measured and analyzed by flow cytometry (EPICS XL, Beckman Coulter Inc., California, USA).

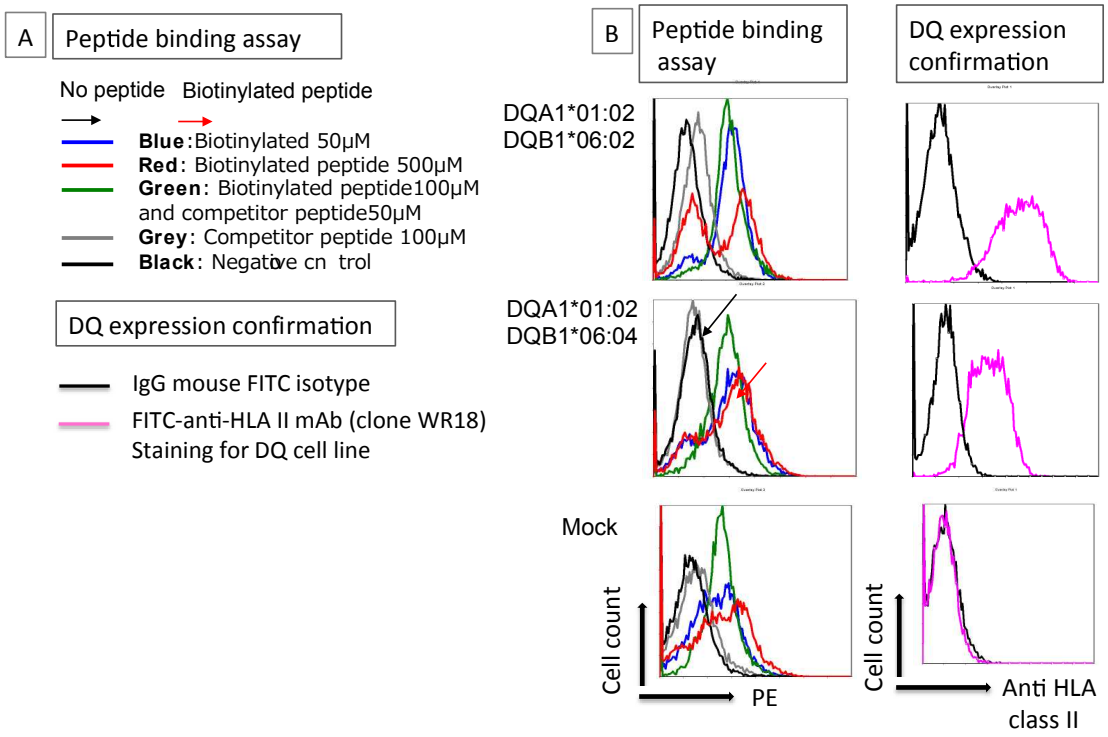

Figure 12. Longer incubation time for binding of insulin $B_{1–15}$ to DQ6 proteins

(A) DQA1*01:02-DQB1*06:02, DQA1*01:02-DQB1*06:04, and mock cells were incubated with insulin $B_{1–15}$ peptide (0–500 μM) for 24 h at 37 °C. DQA1*01:02-DQB1*06:02, DQA1*01:02-DQB1*06:04, and mock cells were collected without trypsinization. DQ*06 protein-expressing NIH3T3 cells were incubated with FITC-conjugated anti-HLA-DR, -DQ, and -DPβ mAb (clone WR18) (Morphosys A.G., Munich, Germany) at 4 °C for 20 min. (B) Flow cytometry signals for insulin $B_{1–15}$ peptide bound to DQA1*01:02-DQB1*06:02 and DQA1*01:02-DQB1*06:04 cells. Biotinylated insulin $B_{1–15}$ peptide was dissolved in 95% DMSO and 5% β-mercaptoethanol. Expression of DQ*06 proteins in NIH3T3 cells was confirmed and analyzed by flow cytometry (EPICS XL, Beckman Coulter Inc., California, USA).

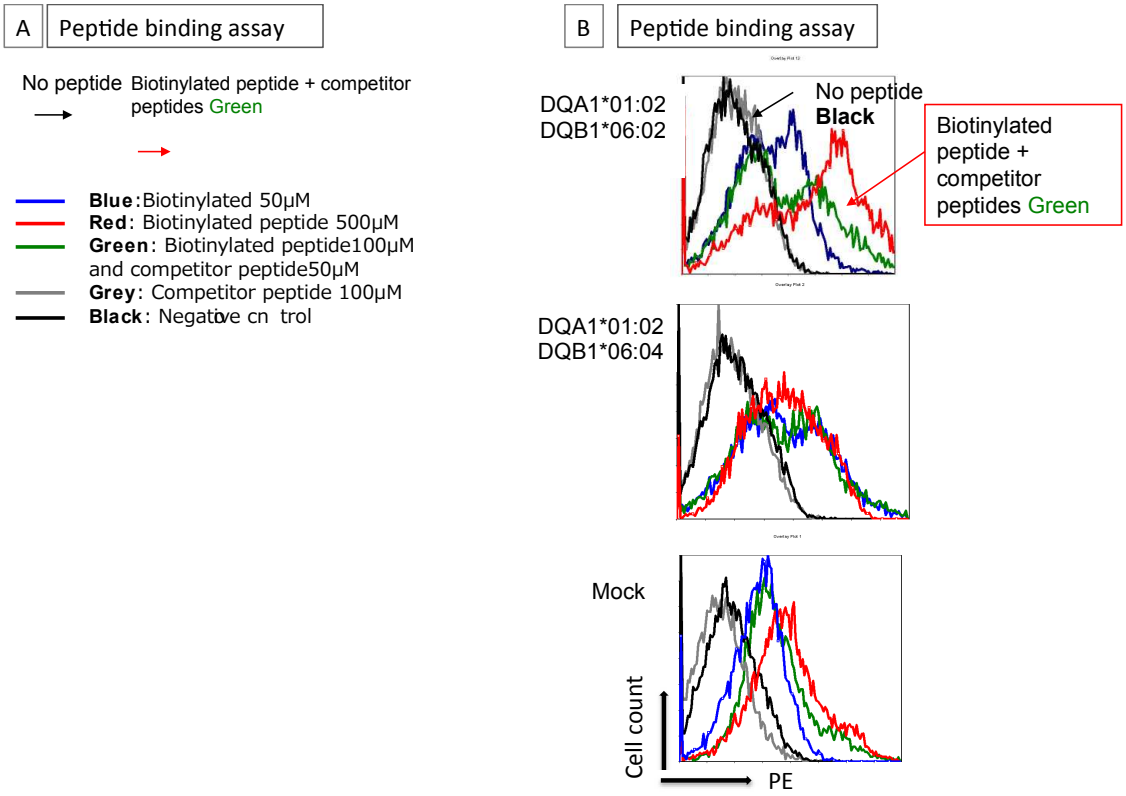

Figure 13. Binding assay of insulin $B_{1–20}$ incubated in plastic tubes

(A) Human insulin $B_{1–20}$ peptide (0–500 μM) was incubated for 4 h in plastic tubes with DQA1*01:02-DQB1*06:02 and mock cells at 37 °C. (B) Flow cytometry signals for insulin $B_{1–20}$ peptide bound to DQA1*01:02-DQB1 *06:02 and mock cells. Biotinylated insulin $B_{1–20}$ peptide was dissolved in 95% DMSO and 5% β-mercaptoethanol. Fluorescence intensities were measured and analyzed by flow cytometry (EPICS XL, Beckman Coulter Inc., California, USA).

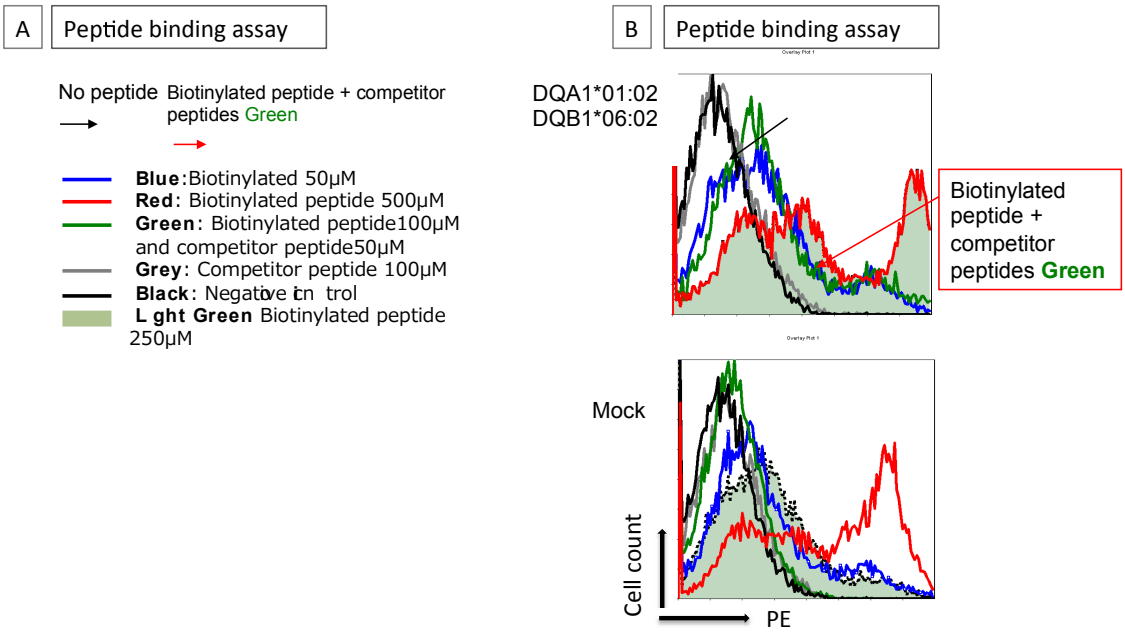

Figure 14. Binding of insulin $B_{1–20}$ to DQ6 protein at a concentration of 500 μM

(A) Human insulin $B_{1–20}$ peptide (0–500 μM) was incubated with DQA1*01:02-DQB1*06:02 or mock cells collected by trypsinization after 24 h in plastic tubes at 37 °C. (B) Flow cytometry signals for insulin $B_{1–20}$ peptide bound to NIH-DQA1*01:02-DQB1*06:02 or mock cells. Biotinylated insulin $B_{1–20}$ peptide was dissolved in 95% DMSO and 5% β-mercaptoethanol. Fluorescence intensities were measured and analyzed by flow cytometry (EPICS XL, Beckman Coulter Inc., California, USA).

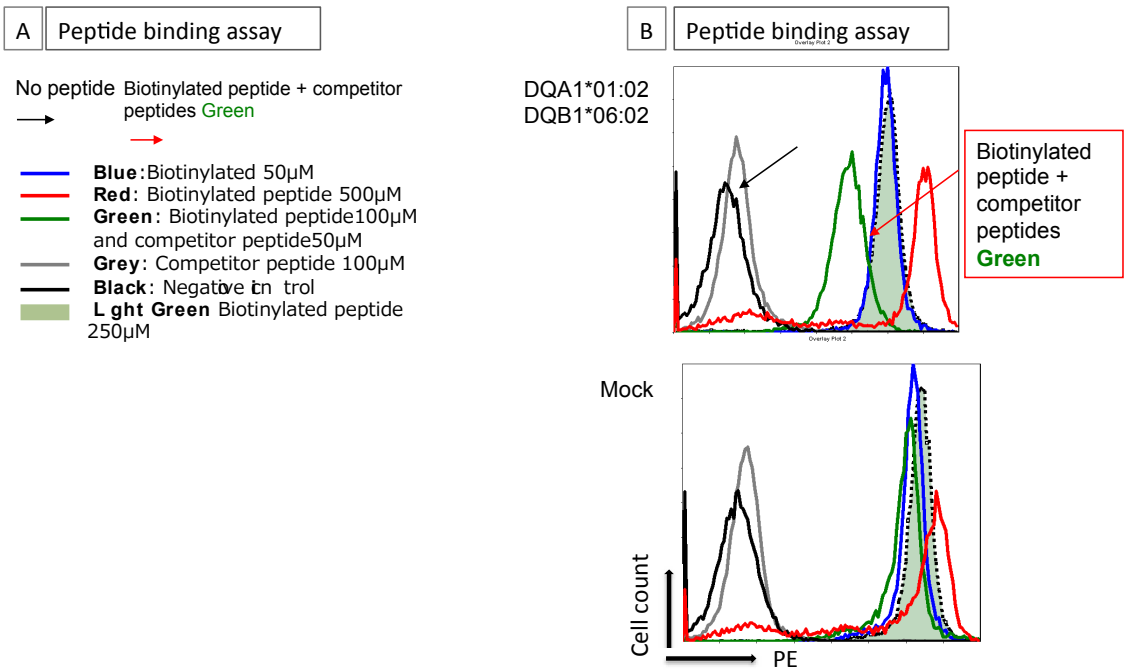

Figure 15. Binding assay of insulin $B_{1–20}$ to DQ6 protein in plastic tubes

(A) DQA1*01:02-DQB1*06:02 and mock cells were collected without trypsinization and were incubated with 0–500 μM human insulin $B_{1–20}$ for 24 h in plastic tubes at 37 °C.

(B) Flow cytometry signals for insulin $B_{1–20}$ peptide bound to DQA1*01:02-DQB1*06:02 or mock cells. Biotinylated insulin $B_{1–20}$ peptide was dissolved in 95% DMSO and 5% β-mercaptoethanol. Fluorescence intensities were measured and analyzed by flow cytometry (EPICS XL, Beckman Coulter Inc., California, USA).

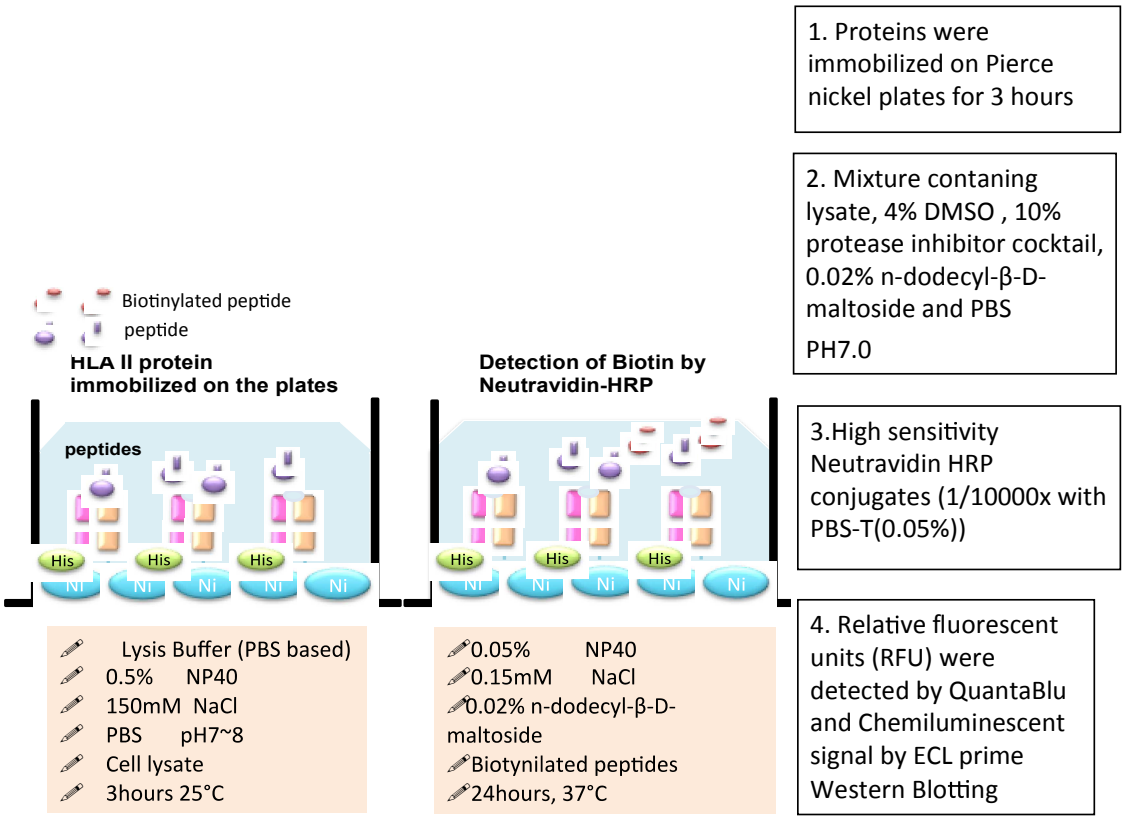

Figure 16. Binding assay of hypocretin peptides to DQ6 proteins

Chemiluminescent signals for hypocretin peptides bound to HLA class II DQ6 proteins. Biotinylated hypocretin peptides were dissolved in 100% DMSO. Various concentrations of hypocretin peptides (0–150 μM) were incubated with HLA class II DQ6 (60 μg) and mock cell lysates (60 μg) at pH 7.0 and 37 °C for 24 h. Subsequently, chemiluminescence signals for hypocretin peptides bound to HLA class II DQ6 proteins were plotted at various concentrations of hypocretin peptides.

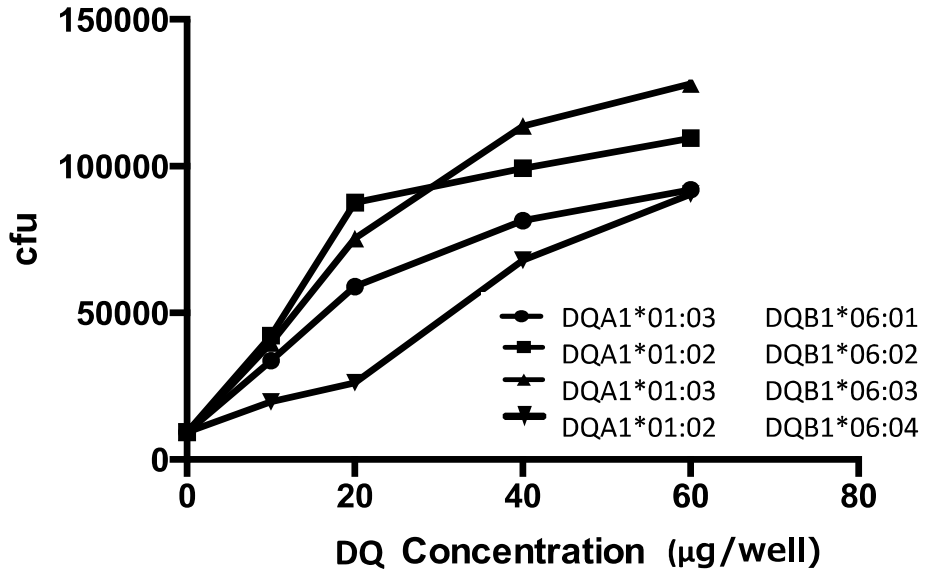

Figure 17. Immobilization of DQ6 protein on Ni^{2+}-coated plates

Chemiluminescent signals were measured to quantify the protein amount of DQA1*01:02-DQB1*06:02 (susceptible haplotype), DQA1*01:03-DQB1*06:01 (resistant), DQA1*01:03-DQB1*06:03 (resistant), or DQA1*01:02-DQB1*06:04 (neutral haplotype) immobilized on the Ni^{2+}-coated plate. Cell lysates (0–60 μg) were applied to each well. DQ proteins were detected using anti-HLA-DR, -DQ, and -DPβ mAbs (clone WR18, 10 μg/mL; Morphosys A.G., Munich, Germany). Chemiluminescence intensities for DQ proteins were detected in each well. Signal intensities were measured by densitometric analysis.

(A)

preprohypocretin

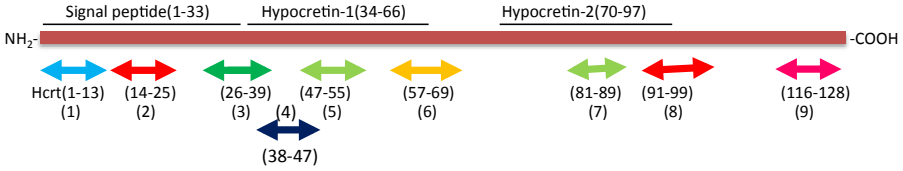

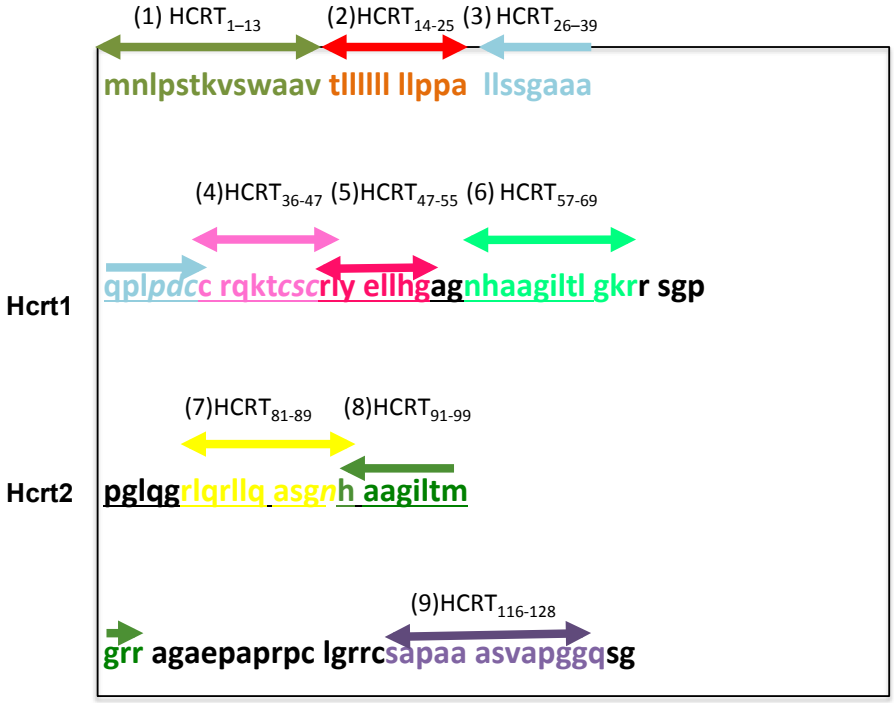

(B)

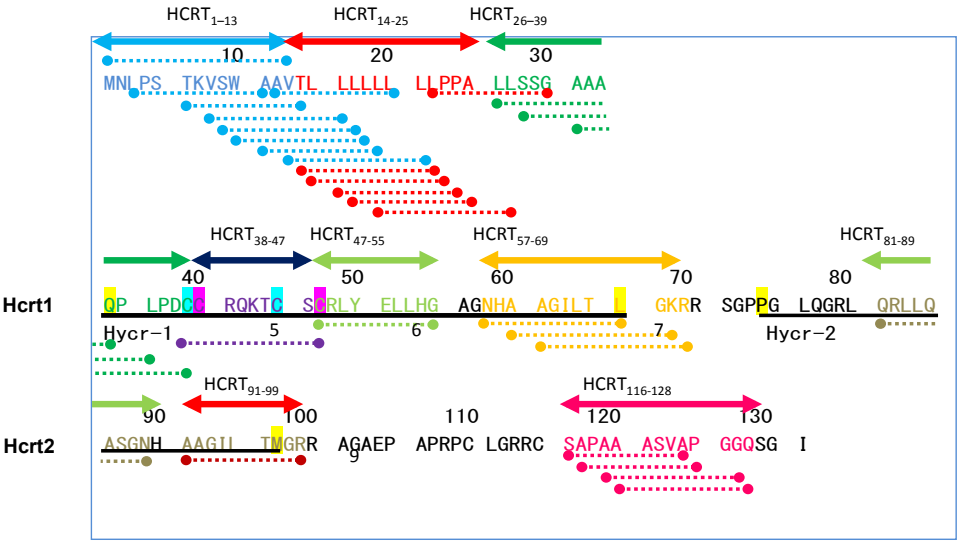

(C)

Potential binding motif for DQB1*06:02

Relative Position	P1	P4	P6	P9
Amino acid	No Basic, No P, No G	No basic, No P	No basic, No acidic, No P, No C	Accept L, I, V (A,P,S,T)

Figure 18. Search for peptide motifs

Hypocretin peptides were designed for nine peptide candidates of hypocretin-1 and hypocretin-2.

(B) The figure shows overlapping hypocretin peptides with the potential binding motif for DQB1*06:02 (66)

(C) The DQA1*0102-DQB1*0602 peptide-binding motif was searched using the software program, TextWrangler. The 13-mer to 15-mer hypocretin peptides were designed on the basis of the previously established 9-mer DQA1*0102-DQB1*0602 binding motif (38).

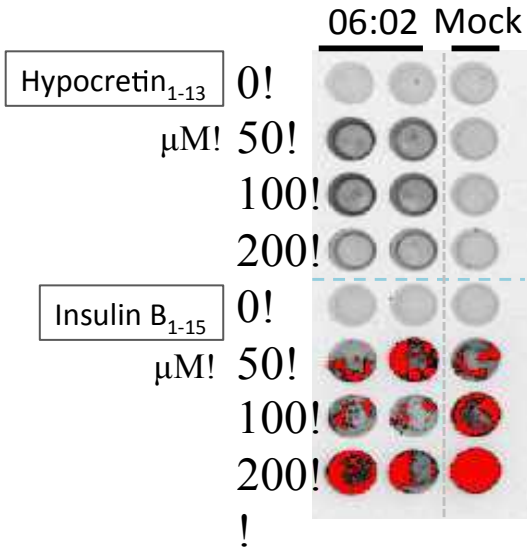

Figure 19. Binding of hypocretin$_{1–13}$ and insulin B$_{1-15}$ peptides to HLA-DQ6 proteins The intensity of chemifluorescence intensities was analyzed using chemiluminescence signals (cfu). Chemiluminescence signals for hypocretin$_{1-13}$ and insulin B$_{1-15}$ peptide bound to DQA1*01:02-DQB1*06:02 proteins were estimated with the ECL™ Reagent and Ni^{2+}-plates (every condition was tested twice). Biotinylated hypocretin$_{1-13}$ and insulin B$_{1-15}$ peptide were dissolved in 100% DMSO. Hypocretin$_{1–13}$ (upper panel) and insulin B$_{1–15}$ peptides (Lower panel; 0–200 µM) were incubated with DQA1*01:02-DQB1*06:02 cell lysates (60 µg) and mock cell lysates (60 µg) at pH 7.0 and 37 °C for 24 h. The figure depicts the Ni^{2+} plate, and chemiluminescence signals were detected by visual inspection. Hypocretin$_{1–13}$ peptide bound to DQA1*01:02-DQB1*06:02 protein, while insulin B$_{1–15}$ peptide bound nonspecifically to mock cell lysates.

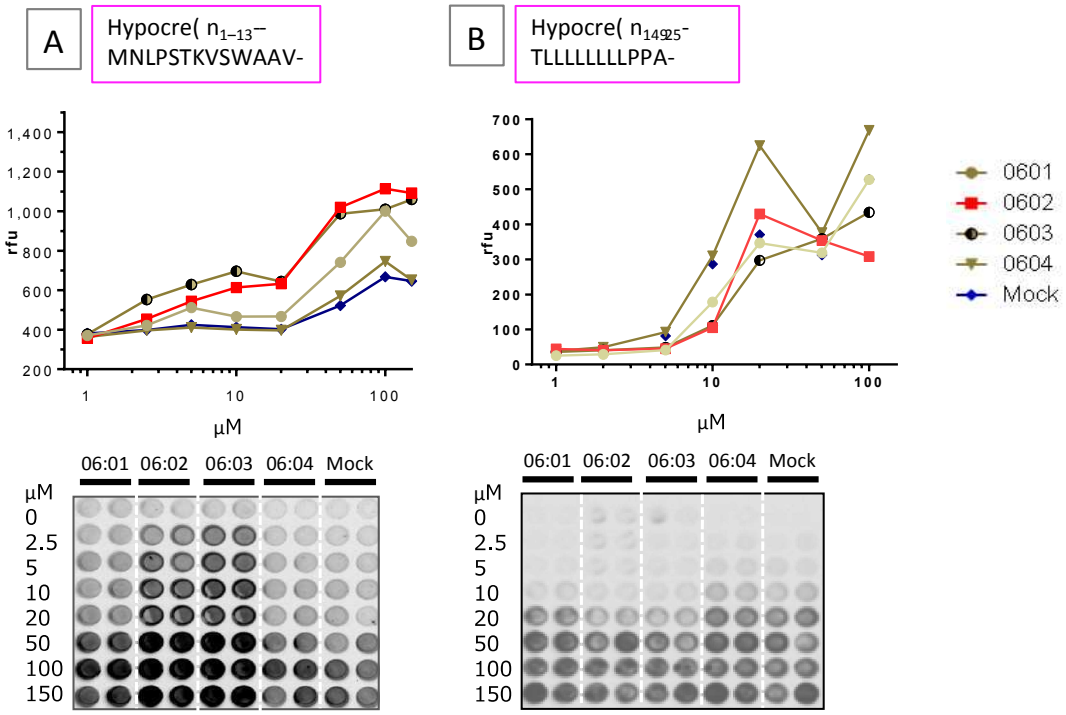

Figure 20. Binding of hypocretin$_{1–13}$ and hypocretin$_{14–25}$ peptides to HLA-DQ6 proteins

For Figures 20–24: Upper panel shows the relative fluorescent intensities (rfu) of signals for hypocretin bound to DQ6 protein, detected using QuantaBlu reagent; Lower panel shows the intensity of chemiluminescence signals for hypocretin peptide bound to DQ6 proteins on Ni^{2+} plate, detected using ECL™ Reagent. Relative fluorescent unit intensity (rfu) for (A) hypocretin$_{1–13}$ and (B) hypocretin$_{14–25}$ peptides bound to DQ6 proteins. Peptides (0–150 μM) were incubated with DQ6 cell lysates (60 μg) or mock cell lysates (60 μg) at pH 7.0 and 37 °C for 24 h. Lower panel shows the Ni^{2+} plate and the intensity of chemiluminescence signals for hypocretin$_{1–13}$ and hypocretin$_{14–25}$ bound to HLA-DQ6 proteins, DQA1*01:02-DQB1*06:02 and DQA1*01:03-DQB1*06:03. The fluorescent intensity of hypocretin peptide on DQ06 cell lysates was fitted to the rfu curve depicted in the upper panel, and the intensity of chemiluminescence signals was estimated by visual inspection and was used to compare the fluorescent intensities of the rfu curve.

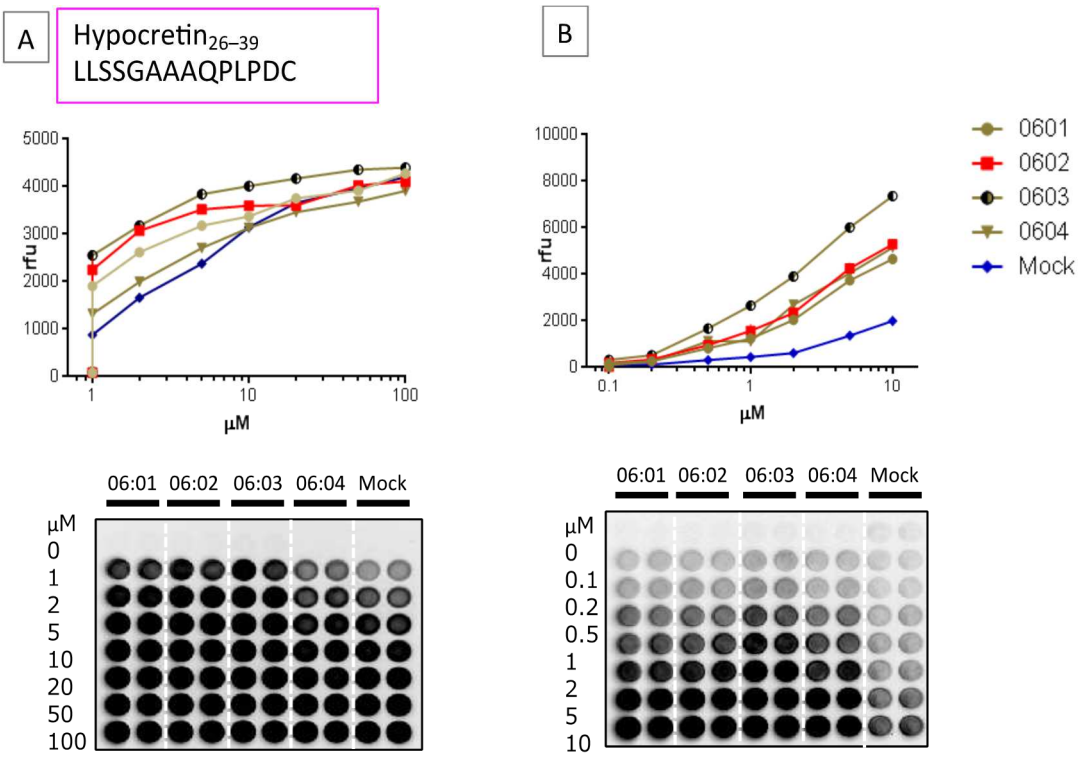

Figure 21. Binding of hypocretin$_{26–39}$ peptides to HLA-DQ6 proteins

Relative fluorescent unit intensity (rfu) and chemiluminescent intensity for hypocretin$_{26–39}$ peptide (A) 0–100 μM or (B) 0–10 μM incubated with DQ6 or mock cell lysates (60 μg) at pH 7.0 and 37 °C for 24 h. Biotinylated hypocretin$_{26–39}$ peptide was dissolved in 100% DMSO. Chemiluminescence signals for hypocretin$_{26–39}$ peptide bound to DQ6 proteins, DQA1*01:03-DQB1*06:01, DQA1*01:02-DQB1*06:02, DQA1*01:03-DQB1* 06:03, and DQA1*01:02-DQB1*06:04, are shown.

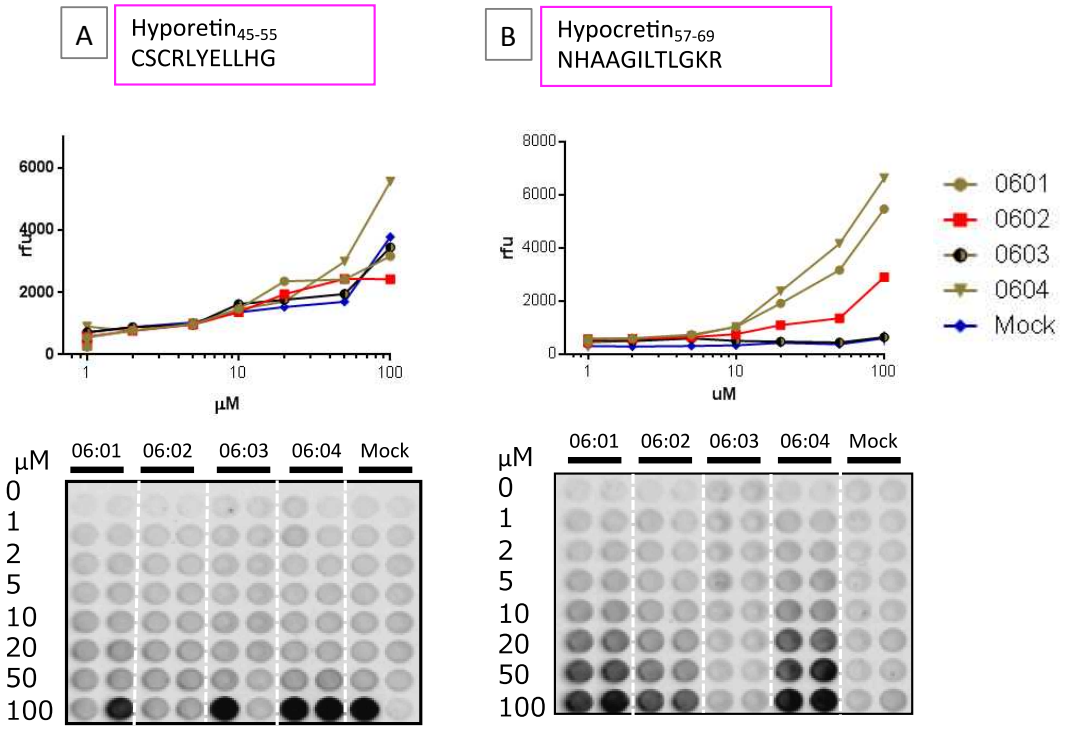

Figure 22. Binding of hypocretin$_{45–55}$ or hypocretin$_{57–69}$ peptides to HLA-DQ6 proteins

Fluorescent intensities and chemiluminescent intensity for (A) hypocretin$_{45–55}$ or (B) hypocretin$_{57–69}$ peptides bound to DQ6 proteins. Biotinylated hypocretin$_{45–55}$ peptide or hypocretin$_{57–69}$ peptide was dissolved in 100% DMSO. Various concentrations of hypocretin$_{45–55}$ or hypocretin$_{57–69}$ (0–100 µM) were incubated with DQ6 cell lysates or mock cell lysates (60 µg) at pH 7.0 and 37 °C for 24 h. Chemiluminescence signals for hypocretin$_{45–55}$ or hypocretin$_{57–69}$ peptide bound to DQ6 proteins are shown.

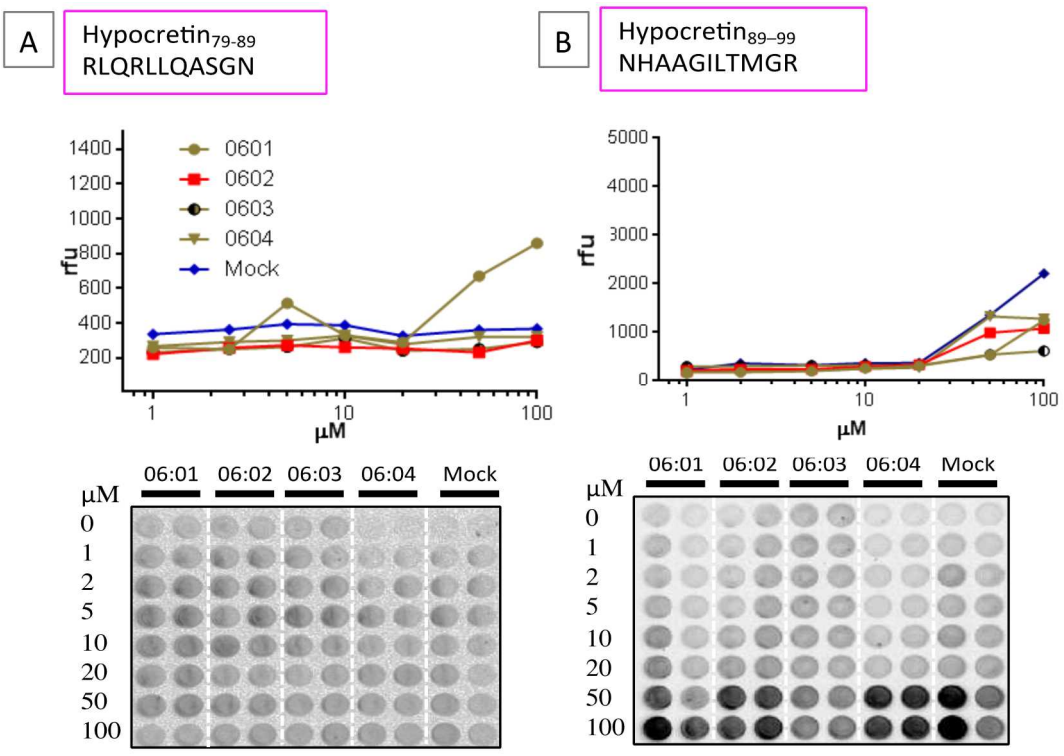

Figure 23. Binding of hypocretin$_{79–89}$ or hypocretin$_{89-99}$ peptides to HLA-DQ6 proteins

Fluorescent intensities and chemiluminescent intensity for (A) hypocretin$_{79–89}$ and (B) hypocretin$_{89-99}$ peptide bound to DQ6 proteins. Biotinylated hypocretin$_{79–89}$ peptide or hypocretin$_{89-99}$ peptide was dissolved in 100% DMSO. Various concentrations of hypocretin$_{79–89}$ or hypocretin$_{89-99}$ (0–100 μM) were incubated with DQ6 cell lysates (60 μg) or mock cell lysates (60 μg) at pH 7.0 and 37 °C for 24 h. Chemiluminescence signals for hypocretin$_{89–89}$ peptide or hypocretin$_{89-99}$ peptide bound to DQ6 are shown.

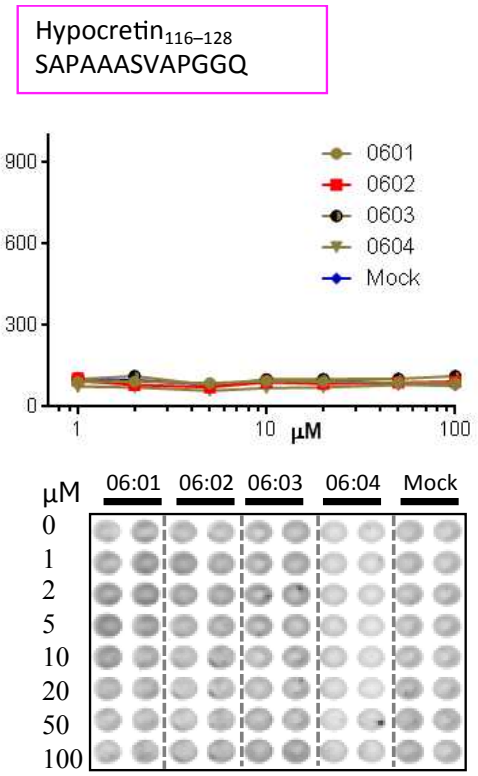

Figure 24 Binding of hypocretin$_{116–128}$ peptides to the DQ6 proteins

Chemiluminescent intensity of hypocretin$_{116–128}$ peptide bound to DQ6 proteins. Biotinylated hypocretin$_{116–128}$ peptide was dissolved in 100% DMSO. Various concentrations of hypocretin$_{116–128}$ peptide (0–100 μM) were incubated with DQ6 cell lysates or mock cell lysates (60 μg) at pH 7.0 and 37 °C for 24 h. Chemiluminescence signals for hypocretin$_{116–128}$ peptide bound to DQ6 proteins are shown.

Table 1. Variants of HLA-DQ1 and HLA-DQ6 proteins

A. DQA1*01

Residues	13β
*DQ *06:01*	A

B. DQB1*06 to MHC pocket

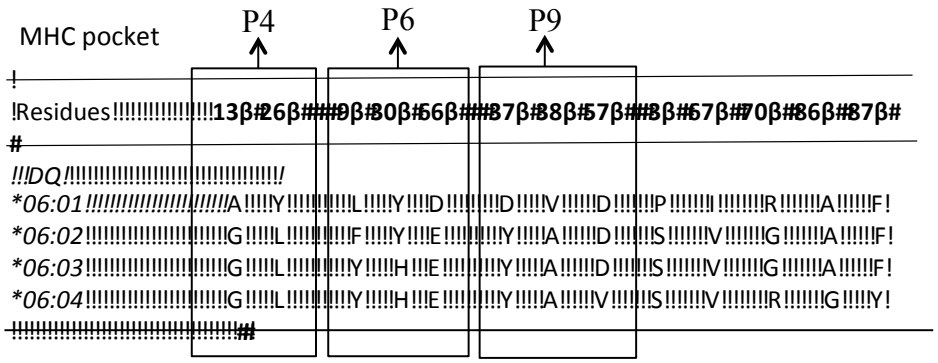

Amino acid residue differences between DQA1*01:02-DQB1*06:02 (susceptible haplotype), DQA1*01:03-DQB1*06:01 (resistant), DQA1*01:03-DQB1*06:03 (resistant), and DQA1*01:02-DQB1*06:04 (neutral haplotype) proteins are indicated in the table.

Table 2. Major narcolepsy resistant and susceptible haplotypes

	DQA1	*DQB1*
Resistant	*DQA1*01:03*	*DQB1*06:01*
	*DQA1*01:03*	*DQB1*06:03*
Susceptible	*DQA1*01:02*	*DQB1*06:02*
Neutral	*DQA1*01:02*	*DQB1*06:04*

References (1, 7)

Table 3. Primers used in this study

	Sequence (5’→3’)
pMxs-puro Fw	5‘-GCCCTCAAAGTAGACGGCATCGC-3’
pMxs-puro Rv	5‘-GTTGCTGACTAATTGAGATGCAGC-3’
pMxs-neo Fw	5‘-TATTTATGCAGAGGCCGAGG-3’
pMxs-neo Rv	5'-GTTCCAGTCCTTGTCTACCTTGTC-3’
48 (DQB1 internal 5’)	5'-ACGGTGTGCAGACACAACTAC-3’
49 (DQB1 internal 3')	5'-CGAAACCACCGGACTTTGATCT-3’
50 (DQA1 internal 5')	5'-ACTCTACCGCTGCTACCAATG-3’
51 (DQA1 internal 3')	5'-TCTAGAAACACCTTCTGTGAC-3’

Table 4. Hypocretin peptides used in this study

Peptide name	Sequence
Hypocretin $_{1-13}$	MNLPSTKVSWAAV
Hypocretin $_{14-25}$	TLLLLLLLLPPA
Hypocretin $_{26-39}$	LLSSGAAAQPLPDC
Hypocretin $_{36-47}$	PDCCRQKTCSC
Hypocretin $_{45-55}$	CSCRLYELLHG
Hypocretin $_{57-69}$	NHAAGILTLGKR
Hypocretin $_{79-89}$	RLQRLLQASGN
Hypocretin $_{89-99}$	NHAAGILTMGR
Hypocretin $_{116-128}$	SAPAAASVAPGGQ

Table 5. Fluorescent intensities of hypocretin$_{1-13}$ and hypocretin$_{14-25}$ peptides

Hypocretin$_{1-13}$

μM	DQA1*01:03-DQB1*06:01#		DQA1*01:02-DQB1*06:02#		DQA1*01:03-DQB1*06:03#		DQA1*01:02-DQB1*06:04#		Mock#	
0	24	26	50	42	64	34	25	32	27	26
1	25	26	47	42	40	32	35	42	35	39
2	29	29	40	41	43	38	46	53	51	45
5	39	43	44	46	47	50	94	91	71	92
10	169	187	95	116	110	112	331	289	253	321
20	334	360	257	602	368	226	612	637	506	235
50	288	349	337	370	386	332	380	373	312	313
100	661	394	360	256	349	520	817	519	285	773

Hypocretin$_{14-25}$

μM	DQA1*01:03-DQB1*06:01#		DQA1*01:02-DQB1*06:02#		DQA1*01:03-DQB1*06:03#		DQA1*01:02-DQB1*06:04#		Mock#	
0	397	344	362	352	379	376	358	367	374	388
2.5	450	394	458	451	552	554	399	395	402	393
5	590	432	606	481	641	615	404	418	435	414
10	481	451	637	590	695	697	389	413	421	404
20	500	435	648	617	625	663	378	415	421	382
50	781	701	1095	943	1006	968	547	595	474	570
100	1007	994	1232	996	1077	943	738	752	697	638
150	826	868	1194	991	1029	1091	554	749	721	571

#; rfu

Table 6. Fluorescent intensities of hypocretin$_{26\text{-}39}$ peptide

Hypocretin$_{26\text{-}39}$

μM	DQA1*01:03-DQB1*06:01#		DQA1*01:02-DQB1*06:02#		DQA1*01:03-DQB1*06:03#		DQA1*01:02-DQB1*06:04#		Mock#	
0	31	30	30	31	37	38	29	29	52	58
0.1	149	188	188	185	310	324	99	99	111	87
0.2	255	277	348	324	510	524	248	248	113	123
0.5	864	777	937	966	1764	1571	1128	1128	264	362
1	1196	1277	1376	1764	2722	2590	1110	1110	451	449
2	2059	2010	2167	2514	4027	3777	2688	2688	545	688
5	3665	3804	4095	4418	6119	5909	4046	4046	1301	1418
10	4566	4737	5145	5434	6720	8003	5144	5144	1847	2138

Hypocretin$_{26\text{-}39}$

μM	DQA1*01:03-DQB1*06:01#		DQA1*01:02-DQB1*06:02#		DQA1*01:03-DQB1*06:03#		DQA1*01:02-DQB1*06:04#		Mock#	
0	80	85	80	84	97	91	77	82	78	82
1	1873	1939	2427	2065	2919	2187	1332	1309	773	983
2	2511	2725	3026	3114	3233	3125	1915	2074	1641	1680
5	3106	3244	3541	3500	3744	3932	2578	2831	2276	2479
10	3242	3501	3550	3645	3926	4093	3114	3146	3171	3116
20	3764	3740	3575	3629	4115	4223	3614	3303	3674	3637
50	3911	3922	3993	4049	4358	4355	3744	3620	3901	4021
100	4254	4303	3967	4256	4477	4322	3968	3854	4127	4280

#; rfu

Table 7. Fluorescent intensities of hypocretin$_{45\text{-}55}$ and hypocretin$_{57\text{-}69}$ peptides

Hypocretin$_{45\text{-}55}$

µM	DQA1*01:03-DQB1*06:01#		DQA1*01:02-DQB1*06:02#		DQA1*01:03-DQB1*06:03#		DQA1*01:02-DQB1*06:04#		Mock#	
0	229	271	259	303	425	450	599	348	436	373
1	558	545	588	575	715	726	1148	659	710	720
2	743	803	759	778	864	903	718	804	833	929
5	991	961	929	1006	888	1043	957	1052	1034	1031
10	1477	1457	1359	1372	1586	1662	1515	1402	1338	1383
20	2230	2486	1943	1943	1732	1794	1690	1722	1433	1624
50	2296	2540	2242	2623	2471	1435	2711	3285	2167	1235
100	2329	4009	2483	2379	5566	1340	5347	5789	6984	592

Hypocretin$_{57\text{-}69}$

µM	DQA1*01:03-DQB1*06:01#		DQA1*01:02-DQB1*06:02#		DQA1*01:03-DQB1*06:03#		DQA1*01:02-DQB1*06:04#		Mock#	
0	443	465	441	427	554	401	288	232	306	321
1	581	585	633	504	604	410	455	410	301	306
2	577	611	616	534	592	384	496	525	284	286
5	704	752	688	581	780	395	625	757	274	335
10	998	1043	819	687	637	360	1036	1030	326	331
20	1935	1886	1192	992	592	354	2537	2188	372	474
50	3091	3239	1349	1349	568	300	3104	5215	330	410
100	4702	6219	2894	2894	745	534	6596	6647	413	775

#; rfu

Table 8. Fluorescent intensities of hypocretin$_{79-89}$ and hypocretin$_{89-99}$ peptides

Hypocretin$_{79-89}$

μM	DQA1*01:03-DQB1*06:01#		DQA1*01:02-DQB1*06:02#		DQA1*01:03-DQB1*06:03#		DQA1*01:02-DQB1*06:04#		Mock#	
0	294	225	233	210	221	240	226	307	296	377
1	250	250	258	259	251	249	252	331	348	379
2.5	690	339	283	263	246	281	267	335	350	439
5	349	311	302	218	327	299	332	325	385	391
10	302	277	244	265	248	232	280	275	313	341
20	910	430	229	234	243	260	312	328	374	346
50	1101	617	288	314	288	293	318	326	359	378
100	294	225	233	210	221	240	226	307	296	377

Hypocretin$_{89-99}$

μM	DQA1*01:03-DQB1*06:01#		DQA1*01:02-DQB1*06:02#		DQA1*01:03-DQB1*06:03#		DQA1*01:02-DQB1*06:04#		Mock#	
0	171	142	159	223	258	268	176	186	191	203
1	200	153	180	250	308	283	188	202	232	223
2	192	164	209	270	306	287	200	205	363	359
5	225	174	194	288	323	302	198	225	308	340
10	326	198	243	345	323	318	244	255	393	338
20	380	232	307	352	327	314	248	294	362	378
50	718	342	1047	932	586	497	1284	1367	1885	825
100	1710	787	893	1262	606	622	1140	1412	3565	856

#; rfu

Table 9. Fluorescent intensities of hypocretin$_{99\text{-}128}$ peptides

Hypocretin$_{99\text{-}128}$

μM	DQA1*01:03-DQB1*06:01#		DQA1*01:02-DQB1*06:02#		DQA1*01:03-DQB1*06:03#		DQA1*01:02-DQB1*06:04#		Mock#	
0	80	98	86	121	101	108	73	74	92	86
1	85	98	85	106	97	106	76	73	99	91
2	90	95	77	83	103	123	71	72	100	95
5	84	90	72	72	76	82	60	58	84	79
10	92	97	82	98	96	107	70	68	95	89
20	89	97	81	88	98	106	73	69	111	86
50	86	91	86	92	102	103	72	89	110	57
100	84	90	89	96	107	119	81	78	111	46

#; rfu

6. REFERENCES

1. Honda, Y., Juji, T., Matsuki, K., Naohara, T., Satake, M., Inoko, H., Someya, T., Harada, S., and Doi, Y. (1986) HLA-DR2 and Dw2 in narcolepsy and in other disorders of excessive somnolence without cataplexy, *Sleep 9*, 133-142.

2. Matsuki, K., Juji, T., Tokunaga, K., Naohara, T., Satake, M., and Honda, Y. (1985) Human histocompatibility leukocyte antigen (HLA) haplotype frequencies estimated from the data on HLA class I, II, and III antigens in 111 Japanese narcoleptics, *J Clin Invest 76*, 2078-2083.

3. Mueller-Eckhardt, G., Meier-Ewert, K., Schendel, D. J., Reinecker, F. B., Multhoff, G., and Mueller-Eckhardt, C. (1986) HLA and narcolepsy in a German population, *Tissue Antigens 28*, 163-169.

4. Juji, T., Satake, M., Honda, Y., and Doi, Y. (1984) HLA antigens in Japanese patients with narcolepsy. All the patients were DR2 positive, *Tissue Antigens 24*, 316-319.

5. Maeda, M., Tamaoka, A., Hayashi, A., Mizusawa, H., and Shoji, S. (1995) [A case of HLA-DR2, DQw1 negative post-traumatic narcolepsy], *Rinsho Shinkeigaku 35*, 811-813.

6. Billiard, M., Seignalet, J., Besset, A., and Cadilhac, J. (1986) HLA-DR2 and narcolepsy, *Sleep 9*, 149-152.

7. Juji, T., Matsuki, K., Tokunaga, K., Naohara, T., and Honda, Y. (1988) Narcolepsy and HLA in the Japanese, *Ann N Y Acad Sci 540*, 106-114.

8. Matsuki, K., Grumet, F. C., Lin, X., Gelb, M., Guilleminault, C., Dement, W. C., and Mignot, E. (1992) DQ (rather than DR) gene marks susceptibility to narcolepsy, *Lancet 339*, 1052.

9. Mignot, E., Lin, L., Rogers, W., Honda, Y., Qiu, X., Lin, X., Okun, M., Hohjoh, H., Miki, T., Hsu, S., Leffell, M., Grumet, F., Fernandez-Vina, M., Honda, M., and Risch, N. (2001) Complex HLA-DR and -DQ interactions confer risk of narcolepsy-cataplexy in three ethnic groups, *Am J Hum Genet 68*, 686-699.

10. Mignot, E. (1994) DQB1*0602 and DQA1*0102(DQ1) are better markers than DR2 for narcolepsy in Caucasian and black Americans., *American Sleep Disorders Association and Sleep Research Society 17:S60-S67*.

11. Hong, S. C., Lin, L., Lo, B., Jeong, J. H., Shin, Y. K., Kim, S. Y., Kweon, Y., Zhang, J., Einen, M., Smith, A., Hansen, J., Grumet, F. C., and Mignot, E. (2007) DQB1*0301 and DQB1*0601 modulate narcolepsy susceptibility in Koreans, *Hum Immunol 68*, 59-68.

12. Hor, H., Kutalik, Z., Dauvilliers, Y., Valsesia, A., Lammers, G. J., Donjacour, C. E., Iranzo, A., Santamaria, J., Peraita Adrados, R., Vicario, J. L., Overeem, S., Arnulf, I., Theodorou, I., Jennum, P., Knudsen, S., Bassetti, C., Mathis, J., Lecendreux, M., Mayer, G., Geisler, P., Beneto, A., Petit, B., Pfister, C., Burki, J. V., Didelot, G., Billiard, M., Ercilla, G., Verduijn, W., Claas, F. H., Vollenweider, P., Waeber, G., Waterworth, D. M., Mooser, V., Heinzer, R., Beckmann, J. S., Bergmann, S., and Tafti, M. (2010) Genome-wide association

study identifies new HLA class II haplotypes strongly protective against narcolepsy, *Nat Genet 42*, 786-789.

13. Han, F., Lin, L., Li, J., Aran, A., Dong, S. X., An, P., Zhao, L., Li, Q. Y., Yan, H., Wang, J. S., Gao, H. Y., Li, M., Gao, Z. C., Strohl, K. P., and Mignot, E. (2012) TCRA, P2RY11, and CPT1B/CHKB associations in Chinese narcolepsy, *Sleep Med 13*, 269-272.

14. Miyagawa, T., Kawashima, M., Nishida, N., Ohashi, J., Kimura, R., Fujimoto, A., Shimada, M., Morishita, S., Shigeta, T., Lin, L., Hong, S. C., Faraco, J., Shin, Y. K., Jeong, J. H., Okazaki, Y., Tsuji, S., Honda, M., Honda, Y., Mignot, E., and Tokunaga, K. (2008) Variant between CPT1B and CHKB associated with susceptibility to narcolepsy, *Nat Genet 40*, 1324-1328.

15. Tafti, M., Petit, B., Chollet, D., Neidhart, E., de Bilbao, F., Kiss, J. Z., Wood, P. A., and Franken, P. (2003) Deficiency in short-chain fatty acid beta-oxidation affects theta oscillations during sleep, *Nat Genet 34*, 320-325.

16. Kornum, B. R., Kawashima, M., Faraco, J., Lin, L., Rico, T. J., Hesselson, S., Axtell, R. C., Kuipers, H., Weiner, K., Hamacher, A., Kassack, M. U., Han, F., Knudsen, S., Li, J., Dong, X., Winkelmann, J., Plazzi, G., Nevsimalova, S., Hong, S. C., Honda, Y., Honda, M., Hogl, B., Ton, T. G., Montplaisir, J., Bourgin, P., Kemlink, D., Huang, Y. S., Warby, S., Einen, M., Eshragh, J. L., Miyagawa, T., Desautels, A., Ruppert, E., Hesla, P. E., Poli, F., Pizza, F., Frauscher, B., Jeong, J. H., Lee, S. P., Strohl, K. P., Longstreth, W. T., Jr., Kvale, M., Dobrovolna, M., Ohayon, M. M., Nepom, G. T., Wichmann, H. E., Rouleau,

G. A., Gieger, C., Levinson, D. F., Gejman, P. V., Meitinger, T., Peppard, P., Young, T., Jennum, P., Steinman, L., Tokunaga, K., Kwok, P. Y., Risch, N., Hallmayer, J., and Mignot, E. (2011) Common variants in P2RY11 are associated with narcolepsy, *Nat Genet 43*, 66-71.

17. Bours, M. J., Swennen, E. L., Di Virgilio, F., Cronstein, B. N., and Dagnelie, P. C. (2006) Adenosine 5'-triphosphate and adenosine as endogenous signaling molecules in immunity and inflammation, *Pharmacol Ther 112*, 358-404.

18. Communi, D., Robaye, B., and Boeynaems, J. M. (1999) Pharmacological characterization of the human P2Y11 receptor, *Br J Pharmacol 128*, 1199-1206.

19. Junger, W. G. (2011) Immune cell regulation by autocrine purinergic signalling, *Nat Rev Immunol 11*, 201-212.

20. Felix, N. J., and Allen, P. M. (2007) Specificity of T-cell alloreactivity, *Nat Rev Immunol 7*, 942-953.

21. van den Hoorn, T., Paul, P., Jongsma, M. L., and Neefjes, J. (2011) Routes to manipulate MHC class II antigen presentation, *Curr Opin Immunol 23*, 88-95.

22. Germain, R. N., and Margulies, D. H. (1993) The biochemistry and cell biology of antigen processing and presentation, *Annu Rev Immunol 11*, 403-450.

23. de Lecea, L., Kilduff, T. S., Peyron, C., Gao, X., Foye, P. E., Danielson, P. E., Fukuhara, C., Battenberg, E. L., Gautvik, V. T., Bartlett, F. S., 2nd, Frankel, W. N., van den Pol, A. N., Bloom, F. E., Gautvik, K. M., and Sutcliffe, J. G. (1998)

The hypocretins: hypothalamus-specific peptides with neuroexcitatory activity, *Proc Natl Acad Sci U S A 95*, 322-327.

24. Sakurai, T., Amemiya, A., Ishii, M., Matsuzaki, I., Chemelli, R. M., Tanaka, H., Williams, S. C., Richarson, J. A., Kozlowski, G. P., Wilson, S., Arch, J. R., Buckingham, R. E., Haynes, A. C., Carr, S. A., Annan, R. S., McNulty, D. E., Liu, W. S., Terrett, J. A., Elshourbagy, N. A., Bergsma, D. J., and Yanagisawa, M. (1998) Orexins and orexin receptors: a family of hypothalamic neuropeptides and G protein-coupled receptors that regulate feeding behavior, *Cell 92*, 1 page following 696.
25. Busby, W. H., Jr., Quackenbush, G. E., Humm, J., Youngblood, W. W., and Kizer, J. S. (1987) An enzyme(s) that converts glutaminyl-peptides into pyroglutamyl-peptides. Presence in pituitary, brain, adrenal medulla, and lymphocytes, *J Biol Chem 262*, 8532-8536.
26. Terao, A., Peyron, C., Ding, J., Wurts, S. W., Edgar, D. M., Heller, H. C., and Kilduff, T. S. (2000) Prepro-hypocretin (prepro-orexin) expression is unaffected by short-term sleep deprivation in rats and mice, *Sleep 23*, 867-874.
27. Taheri, S., Sunter, D., Dakin, C., Moyes, S., Seal, L., Gardiner, J., Rossi, M., Ghatei, M., and Bloom, S. (2000) Diurnal variation in orexin A immunoreactivity and prepro-orexin mRNA in the rat central nervous system, *Neurosci Lett 279*, 109-112.
28. Sakurai, T. (2014) The role of orexin in motivated behaviours, *Nat Rev Neurosci 15*, 719-731.

29. Thannickal, T. C., Moore, R. Y., Nienhuis, R., Ramanathan, L., Gulyani, S., Aldrich, M., Cornford, M., and Siegel, J. M. (2000) Reduced number of hypocretin neurons in human narcolepsy, *Neuron 27*, 469-474.

30. Bourgin, P., Huitron-Resendiz, S., Spier, A. D., Fabre, V., Morte, B., Criado, J. R., Sutcliffe, J. G., Henriksen, S. J., and de Lecea, L. (2000) Hypocretin-1 modulates rapid eye movement sleep through activation of locus coeruleus neurons, *J Neurosci 20*, 7760-7765.

31. Mignot, E., Lammers, G. J., Ripley, B., Okun, M., Nevsimalova, S., Overeem, S., Vankova, J., Black, J., Harsh, J., Bassetti, C., Schrader, H., and Nishino, S. (2002) The role of cerebrospinal fluid hypocretin measurement in the diagnosis of narcolepsy and other hypersomnias, *Arch Neurol 59*, 1553-1562.

32. Parkes, J. D., Langdon, N., and Lock, C. (1986) Narcolepsy and immunity, *Br Med J (Clin Res Ed) 292*, 359-360.

33. Thompson, M. D., Comings, D. E., Abu-Ghazalah, R., Jereseh, Y., Lin, L., Wade, J., Sakurai, T., Tokita, S., Yoshida, T., Tanaka, H., Yanagisawa, M., Burnham, W. M., and Moldofsky, H. (2004) Variants of the orexin2/hcrt2 receptor gene identified in patients with excessive daytime sleepiness and patients with Tourette's syndrome comorbidity, *Am J Med Genet B Neuropsychiatr Genet 129B*, 69-75.

34. Aldrich, M. S., and Reynolds, P. R. (1999) Narcolepsy and the hypocretin receptor 2 gene, *Neuron 23*, 625-626.

35. Nishino, S. (2003) The hypocretin/orexin system in health and disease, *Biol Psychiatry 54*, 87-95.

36. Nishino, S., Ripley, B., Overeem, S., Lammers, G. J., and Mignot, E. (2000) Hypocretin (orexin) deficiency in human narcolepsy, *Lancet 355*, 39-40.

37. Mignot, E., Tafti, M., Dement, W. C., and Grumet, F. C. (1995) Narcolepsy and immunity, *Adv Neuroimmunol 5*, 23-37.

38. Siebold, C., Hansen, B. E., Wyer, J. R., Harlos, K., Esnouf, R. E., Svejgaard, A., Bell, J. I., Strominger, J. L., Jones, E. Y., and Fugger, L. (2004) Crystal structure of HLA-DQ0602 that protects against type 1 diabetes and confers strong susceptibility to narcolepsy, *Proc Natl Acad Sci U S A 101*, 1999-2004.

39. Nishino, S., Okuro, M., Kotorii, N., Anegawa, E., Ishimaru, Y., Matsumura, M., and Kanbayashi, T. (2010) Hypocretin/orexin and narcolepsy: new basic and clinical insights, *Acta Physiol (Oxf) 198*, 209-222.

40. Arii, J., Kanbayashi, T., Tanabe, Y., Sawaishi, Y., Kimura, S., Watanabe, A., Mishima, K., Hishikawa, Y., Shimizu, T., and Nishino, S. (2004) CSF hypocretin-1 (orexin-A) levels in childhood narcolepsy and neurologic disorders, *Neurology 63*, 2440-2442.

41. Fontana, A., Gast, H., Reith, W., Recher, M., Birchler, T., and Bassetti, C. L. (2010) Narcolepsy: autoimmunity, effector T cell activation due to infection, or T cell independent, major histocompatibility complex class II induced neuronal loss?, *Brain 133*, 1300-1311.

42. Black, J. L., 3rd, Silber, M. H., Krahn, L. E., Fredrickson, P. A., Pankratz, V. S., Avula, R., Walker, D. L., and Slocumb, N. L. (2005) Analysis of hypocretin (orexin) antibodies in patients with narcolepsy, *Sleep 28*, 427-431.

43. Tanaka, S., Honda, Y., Inoue, Y., and Honda, M. (2006) Detection of autoantibodies against hypocretin, hcrtrl, and hcrtr2 in narcolepsy: anti-Hcrt system antibody in narcolepsy, *Sleep 29*, 633-638.

44. Smith, A. J., Jackson, M. W., Neufing, P., McEvoy, R. D., and Gordon, T. P. (2004) A functional autoantibody in narcolepsy, *Lancet 364*, 2122-2124.

45. Billiard, M. (1985) Narcolepsy. Clinical features and aetiology, *Ann Clin Res 17*, 220-226.

46. Aran, A., Lin, L., Nevsimalova, S., Plazzi, G., Hong, S. C., Weiner, K., Zeitzer, J., and Mignot, E. (2009) Elevated anti-streptococcal antibodies in patients with recent narcolepsy onset, *Sleep 32*, 979-983.

47. Khairkar, P., and Diwan, S. (2012) Late-onset obsessive-compulsive disorder with comorbid narcolepsy after perfect blend of thalamo-striatal stroke and post-streptococcal infection, *J Neuropsychiatry Clin Neurosci 24*, E29-31.

48. Longstreth, W. T., Jr., Ton, T. G., and Koepsell, T. D. (2009) Narcolepsy and streptococcal infections, *Sleep 32*, 1548.

49. Natarajan, N., Jain, S. V., Chaudhry, H., Hallinan, B. E., and Simakajornboon, N. (2013) Narcolepsy-cataplexy: is streptococcal infection a trigger?, *J Clin Sleep Med 9*, 269-270.

50. Cvetkovic-Lopes, V., Bayer, L., Dorsaz, S., Maret, S., Pradervand, S., Dauvilliers, Y., Lecendreux, M., Lammers, G. J., Donjacour, C. E., Du Pasquier, R. A., Pfister, C., Petit, B., Hor, H., Muhlethaler, M., and Tafti, M. (2010) Elevated Tribbles homolog 2-specific antibody levels in narcolepsy patients, *J Clin Invest 120*, 713-719.

51. Toyoda, H., Tanaka, S., Miyagawa, T., Honda, Y., Tokunaga, K., and Honda, M. (2010) Anti-Tribbles homolog 2 autoantibodies in Japanese patients with narcolepsy, *Sleep 33*, 875-878.

52. Ahmed, S. S., Schur, P. H., MacDonald, N. E., and Steinman, L. (2014) Narcolepsy, 2009 A(H1N1) pandemic influenza, and pandemic influenza vaccinations: what is known and unknown about the neurological disorder, the role for autoimmunity, and vaccine adjuvants, *J Autoimmun 50*, 1-11.

53. Barker, C. I., and Snape, M. D. (2014) Pandemic influenza A H1N1 vaccines and narcolepsy: vaccine safety surveillance in action, *Lancet Infect Dis 14*, 227-238.

54. Dauvilliers, Y., Arnulf, I., Lecendreux, M., Monaca Charley, C., Franco, P., Drouot, X., d'Ortho, M. P., Launois, S., Lignot, S., Bourgin, P., Nogues, B., Rey, M., Bayard, S., Scholz, S., Lavault, S., Tubert-Bitter, P., Saussier, C., Pariente, A., and Narcoflu, V. F. s. g. (2013) Increased risk of narcolepsy in children and adults after pandemic H1N1 vaccination in France, *Brain 136*, 2486-2496.

55. Eurosurveillance editorial, t. (2010) European Medicines Agency updates on the review of Pandemrix and reports of narcolepsy, *Euro Surveill 15*.

56. Miller, E., Andrews, N., Stellitano, L., Stowe, J., Winstone, A. M., Shneerson, J., and Verity, C. (2013) Risk of narcolepsy in children and young people receiving AS03 adjuvanted pandemic A/H1N1 2009 influenza vaccine: retrospective analysis, *BMJ 346*, f794.

57. Nohynek, H., Jokinen, J., Partinen, M., Vaarala, O., Kirjavainen, T., Sundman, J., Himanen, S. L., Hublin, C., Julkunen, I., Olsen, P., Saarenpaa-Heikkila, O., and Kilpi, T. (2012) AS03 adjuvanted AH1N1 vaccine associated with an abrupt increase in the incidence of childhood narcolepsy in Finland, *PLoS One 7*, e33536.

58. Partinen, M., Kornum, B. R., Plazzi, G., Jennum, P., Julkunen, I., and Vaarala, O. (2014) Narcolepsy as an autoimmune disease: the role of H1N1 infection and vaccination, *Lancet Neurol 13*, 600-613.

59. van der Most, R., Van Mechelen, M., Destexhe, E., Wettendorff, M., and Hanon, E. (2013) Narcolepsy and A(H1N1)pdm09 vaccination: Shaping the research on the observed signal, *Hum Vaccin Immunother 10*.

60. Widgren, K., Magnusson, M., Hagstam, P., Widerstrom, M., Ortqvist, A., Einemo, I. M., Follin, P., Lindblom, A., Makitalo, S., Wik, O., Osterlund, A., Grunewald, M., Uhnoo, I., and Linde, A. (2013) Prevailing effectiveness of the 2009 influenza A(H1N1)pdm09 vaccine during the 2010/11 season in Sweden, *Euro Surveill 18*, 20447.

61. Wijnans, L., Lecomte, C., de Vries, C., Weibel, D., Sammon, C., Hviid, A., Svanstrom, H., Molgaard-Nielsen, D., Heijbel, H., Dahlstrom, L. A., Hallgren,

J., Sparen, P., Jennum, P., Mosseveld, M., Schuemie, M., van der Maas, N., Partinen, M., Romio, S., Trotta, F., Santuccio, C., Menna, A., Plazzi, G., Moghadam, K. K., Ferro, S., Lammers, G. J., Overeem, S., Johansen, K., Kramarz, P., Bonhoeffer, J., and Sturkenboom, M. C. (2013) The incidence of narcolepsy in Europe: before, during, and after the influenza A(H1N1)pdm09 pandemic and vaccination campaigns, *Vaccine 31*, 1246-1254.

62. Newell, E. W. (2013) Higher throughput methods of identifying T cell epitopes for studying outcomes of altered antigen processing and presentation, *Front Immunol 4*, 430.

63. Buckner, J., Kwok, W. W., Nepom, B., and Nepom, G. T. (1996) Modulation of HLA-DQ binding properties by differences in class II dimer stability and pH-dependent peptide interactions, *J Immunol 157*, 4940-4945.

64. Kwok, W. W., Domeier, M. L., Raymond, F. C., Byers, P., and Nepom, G. T. (1996) Allele-specific motifs characterize HLA-DQ interactions with a diabetes-associated peptide derived from glutamic acid decarboxylase, *J Immunol 156*, 2171-2177.

65. Nepom, B. S., Nepom, G. T., Coleman, M., and Kwok, W. W. (1996) Critical contribution of beta chain residue 57 in peptide binding ability of both HLA-DR and -DQ molecules, *Proc Natl Acad Sci U S A 93*, 7202-7206.

66. Ettinger, R. A., and Kwok, W. W. (1998) A peptide binding motif for HLA-DQA1*0102/DQB1*0602, the class II MHC molecule associated with

dominant protection in insulin-dependent diabetes mellitus, *J Immunol 160*, 2365-2373.

67. Drouin, E. E., Glickstein, L., Kwok, W. W., Nepom, G. T., and Steere, A. C. (2008) Human homologues of a Borrelia T cell epitope associated with antibiotic-refractory Lyme arthritis, *Mol Immunol 45*, 180-189.

68. Bieganowska, K., Hollsberg, P., Buckle, G. J., Lim, D. G., Greten, T. F., Schneck, J., Altman, J. D., Jacobson, S., Ledis, S. L., Hanchard, B., Chin, J., Morgan, O., Roth, P. A., and Hafler, D. A. (1999) Direct analysis of viral-specific CD8+ T cells with soluble HLA-A2/Tax11-19 tetramer complexes in patients with human T cell lymphotropic virus-associated myelopathy, *J Immunol 162*, 1765-1771.

69. Kessler, J. H., Benckhuijsen, W. E., Mutis, T., Melief, C. J., van der Burg, S. H., and Drijfhout, J. W. (2004) Competition-based cellular peptide binding assay for HLA class I, *Curr Protoc Immunol Chapter 18*, Unit 18 12.

70. Hammer, J., Bono, E., Gallazzi, F., Belunis, C., Nagy, Z., and Sinigaglia, F. (1994) Precise prediction of major histocompatibility complex class II-peptide interaction based on peptide side chain scanning, *J Exp Med 180*, 2353-2358.

71. Buus, S., Lise Lauemoller, S., Stryhn, A., and Ostergaard Pedersen, L. (2001) Measurement of peptide-MHC interactions in solution using the spin column filtration assay, *Curr Protoc Immunol Chapter 18*, Unit 18 14.

72. Kessler, J. H., Mommaas, B., Mutis, T., Huijbers, I., Vissers, D., Benckhuijsen, W. E., Schreuder, G. M., Offringa, R., Goulmy, E., Melief, C. J., van der Burg, S.

H., and Drijfhout, J. W. (2003) Competition-based cellular peptide binding assays for 13 prevalent HLA class I alleles using fluorescein-labeled synthetic peptides, *Hum Immunol 64*, 245-255.

73. Margulies, D. H., Corr, M., Boyd, L. F., and Khilko, S. N. (1993) MHC class I/peptide interactions: binding specificity and kinetics, *J Mol Recognit 6*, 59-69.

74. Hammer, J., Belunis, C., Bolin, D., Papadopoulos, J., Walsky, R., Higelin, J., Danho, W., Sinigaglia, F., and Nagy, Z. A. (1994) High-affinity binding of short peptides to major histocompatibility complex class II molecules by anchor combinations, *Proc Natl Acad Sci U S A 91*, 4456-4460.

75. Ettinger, R. A., Papadopoulos, G. K., Moustakas, A. K., Nepom, G. T., and Kwok, W. W. (2006) Allelic variation in key peptide-binding pockets discriminates between closely related diabetes-protective and diabetes-susceptible HLA-DQB1*06 alleles, *J Immunol 176*, 1988-1998.

76. Morita, S., Kojima, T., and Kitamura, T. (2000) Plat-E: an efficient and stable system for transient packaging of retroviruses, *Gene Ther 7*, 1063-1066.

77. Landi, S., Ciucci, F., Maffei, L., Berardi, N., and Cenni, M. C. (2009) Setting the pace for retinal development: environmental enrichment acts through insulin-like growth factor 1 and brain-derived neurotrophic factor, *J Neurosci 29*, 10809-10819.

78. Chen, A. K., Behlke, M. A., and Tsourkas, A. (2008) Efficient cytosolic delivery of molecular beacon conjugates and flow cytometric analysis of target RNA, *Nucleic Acids Res 36*, e69.

79. Ikeda, H., Kato, K., Suzuki, T., Kitani, H., Matsubara, Y., Takase-Yoden, S., Watanabe, R., Kitagawa, M., and Aizawa, S. (2000) Properties of the naturally occurring soluble surface glycoprotein of ecotropic murine leukemia virus: binding specificity and possible conformational change after binding to receptor, *J Virol 74*, 1815-1826.

80. Ignatowski, T. A., and Bidlack, J. M. (1998) Detection of kappa opioid receptors on mouse thymocyte phenotypic subpopulations as assessed by flow cytometry, *J Pharmacol Exp Ther 284*, 298-306.

81. Bucher, M. H., Evdokimov, A. G., and Waugh, D. S. (2002) Differential effects of short affinity tags on the crystallization of Pyrococcus furiosus maltodextrin-binding protein, *Acta Crystallogr D Biol Crystallogr 58*, 392-397.

82. Rothbard, J. B., and Busch, R. (2001) Binding of biotinylated peptides to MHC class II proteins on cell surfaces, *Curr Protoc Immunol Chapter 18*, Unit 18 11.

83. Lee, K. H., Wucherpfennig, K. W., and Wiley, D. C. (2001) Structure of a human insulin peptide-HLA-DQ8 complex and susceptibility to type 1 diabetes, *Nat Immunol 2*, 501-507.

84. Nepom, G. T., and Kwok, W. W. (1998) Molecular basis for HLA-DQ associations with IDDM, *Diabetes 47*, 1177-1184.

85. De la Herran-Arita, A. K., Kornum, B. R., Mahlios, J., Jiang, W., Lin, L., Hou, T. Y., Macaubas, C., Einen, M., Plazzi, G., Crowe, C., Newell, E. W., Davis, M. M., Mellins, E. D., and Mignot, E. (2013) CD4(+) T Cell Autoimmunity to

Hypocretin/Orexin and Cross-Reactivity to a 2009 H1N1 Influenza A Epitope in Narcolepsy, *Science Translational Medicine 5*.

86. De la Herran-Arita, A. K., and Garcia-Garcia, F. (2014) Narcolepsy as an immune-mediated disease, *Sleep Disord 2014*, 792687.

87. De la Herran-Arita, A. K., Kornum, B. R., Mahlios, J., Jiang, W., Lin, L., Hou, T., Macaubas, C., Einen, M., Plazzi, G., Crowe, C., Newell, E. W., Davis, M. M., Mellins, E. D., and Mignot, E. (2014) Retraction of the research article: "CD4(+) T cell autoimmunity to hypocretin/orexin and cross-reactivity to a 2009 H1N1 influenza A epitope in narcolepsy", *Sci Transl Med 6*, 247rt241.

88. Steward-Tharp, S. M., Song, Y. J., Siegel, R. M., and O'Shea, J. J. (2010) New insights into T cell biology and T cell-directed therapy for autoimmunity, inflammation, and immunosuppression, *Ann N Y Acad Sci 1183*, 123-148.

89. Blouin, A. M., Thannickal, T. C., Worley, P. F., Baraban, J. M., Reti, I. M., and Siegel, J. M. (2005) Narp immunostaining of human hypocretin (orexin) neurons: loss in narcolepsy, *Neurology 65*, 1189-1192.

90. Crocker, A., Espana, R. A., Papadopoulou, M., Saper, C. B., Faraco, J., Sakurai, T., Honda, M., Mignot, E., and Scammell, T. E. (2005) Concomitant loss of dynorphin, NARP, and orexin in narcolepsy, *Neurology 65*, 1184-1188.

91. Lin, W. Y., and Roberts, M. R. (2002) Developmental dissociation of T cells from B, NK, and myeloid cells revealed by MHC class II-specific chimeric immune receptors bearing TCR-zeta or FcR-gamma chain signaling domains, *Blood 100*, 3045-3048.

92. Al-Ghouti, M. A., Khraisheh, M. A., Ahmad, M. N., and Allen, S. J. (2007) Microcolumn studies of dye adsorption onto manganese oxides modified diatomite, *J Hazard Mater 146*, 316-327.

7. ACKNOWLEDGMENTS

I thank Dr. Hiroko Miyadera and Professor Katsushi Tokunaga (Department of Human Genetics, Graduate School of Medicine, University of Tokyo) for supervision of this project, Associate Professor Akihiko Mabuchi and Assistant Professor Taku Miyagawa (Department of Human Genetics, Graduate School of Medicine, University of Tokyo) for the insightful comments, suggestions and for the time.

I thank Yuki Uchida for establishing stimulation condition of HLA class II in NIH 3T3 cell, Cindy Chen for development of plate-based peptide binding assay, and all of the members of the Department of Human Genetics, Graduate School of Medicine, University of Tokyo.